

AWARD NUMBER: W81XWH-15-1-0160

TITLE:

Cyclin E1 as a Therapeutic Target in Women with High-Grade Serous Ovarian Cancer and Primary Treatment Failure

PRINCIPAL INVESTIGATOR: Professor David Bowtell, PhD

CONTRACTING ORGANIZATION: University of Melbourne

Parkville , Victoria 3052 Australia

REPORT DATE: September 2016

TYPE OF REPORT: Annual

PREPARED FOR: U.S. Army Medical Research and Materiel Command
Fort Detrick, Maryland 21702-5012

DISTRIBUTION STATEMENT: Approved for Public Release;
Distribution Unlimited

The views, opinions and/or findings contained in this report are those of the author(s) and should not be construed as an official Department of the Army position, policy or decision unless so designated by other documentation.

REPORT DOCUMENTATION PAGE				Form Approved OMB No. 0704-0188	
Public reporting burden for this collection of information is estimated to average 1 hour per response, including the time for reviewing instructions, searching existing data sources, gathering and maintaining the data needed, and completing and reviewing this collection of information. Send comments regarding this burden estimate or any other aspect of this collection of information, including suggestions for reducing this burden to Department of Defense, Washington Headquarters Services, Directorate for Information Operations and Reports (0704-0188), 1215 Jefferson Davis Highway, Suite 1204, Arlington, VA 22202-4302. Respondents should be aware that notwithstanding any other provision of law, no person shall be subject to any penalty for failing to comply with a collection of information if it does not display a currently valid OMB control number. PLEASE DO NOT RETURN YOUR FORM TO THE ABOVE ADDRESS.					
1. REPORT DATE September 2016		2. REPORT TYPE Annual		3. DATES COVERED 1 Sep 2015 - 31 Aug 2016	
4. TITLE AND SUBTITLE Cyclin E1 as a Therapeutic Target in Women with High-Grade Serous Ovarian Cancer and Primary Treatment Failure				5a. CONTRACT NUMBER	
				5b. GRANT NUMBER W81XWH-15-1-0160	
				5c. PROGRAM ELEMENT NUMBER	
6. AUTHOR(S) David Bowtell, PhD Jessica Beach, PhD E-Mail: david.bowtell@petermac.org ; jessica.beach@petermac.org				5d. PROJECT NUMBER	
				5e. TASK NUMBER	
				5f. WORK UNIT NUMBER	
7. PERFORMING ORGANIZATION NAME(S) AND ADDRESS(ES) University of Melbourne Parkville, Victoria 3052 Australia				8. PERFORMING ORGANIZATION REPORT NUMBER	
9. SPONSORING / MONITORING AGENCY NAME(S) AND ADDRESS(ES) U.S. Army Medical Research and Materiel Command Fort Detrick, Maryland 21702-5012				10. SPONSOR/MONITOR'S ACRONYM(S)	
				11. SPONSOR/MONITOR'S REPORT NUMBER(S)	
12. DISTRIBUTION / AVAILABILITY STATEMENT Approved for Public Release; Distribution Unlimited					
13. SUPPLEMENTARY NOTES					
14. ABSTRACT A significant number of women with high-grade serous ovarian cancer (HGSC) are intrinsically refractory to standard platinum-based treatment. We have previously shown that amplification of the cyclin E1 gene (<i>CCNE1</i>) in HGSC is associated with primary chemoresistance and poor clinical outcome. Therefore, we hypothesized that cyclin E1 is a key therapeutic target in HGSC, and that generation of a genetically engineered mouse (GEM) model of <i>CCNE1</i> -amplified HGSC will facilitate the development of novel therapeutic strategies. Here, we have generated two mouse strains with Cre-mediated expression of full-length or truncated <i>Ccne1</i> at the <i>Rosa26</i> locus. We plan to cross these mice with <i>Pax8-TetOCre-Tp53</i> mice in order to induce expression of <i>Ccne1</i> in the fallopian tube epithelium and drive the initiation and development of HGSC. Mouse models that closely resemble human disease have been powerful platforms for new therapies and understanding resistance mechanisms. Immune checkpoint inhibitors have shown substantial activity in melanoma and lung cancer, and it is now a priority to extend these findings to other solid cancers, including HGSC. The availability of an intact animal model of <i>CCNE1</i> is likely to be a substantial value in development of immune checkpoint inhibitors and other approaches to targeting <i>CCNE1</i> amplified tumours.					
15. SUBJECT TERMS Cyclin E1, CCNE1, amplification, genomic instability, high-grade serous ovarian cancer (HGSC), chemoresistance, mouse models, fallopian tube, homologous recombination (HR)					
16. SECURITY CLASSIFICATION OF:			17. LIMITATION OF ABSTRACT Unclassified	18. NUMBER OF PAGES 34	19a. NAME OF RESPONSIBLE PERSON USAMRMC
a. REPORT Unclassified	b. ABSTRACT Unclassified	c. THIS PAGE Unclassified			19b. TELEPHONE NUMBER (include area code)

Table of Contents

	<u>Page</u>
1. Introduction.....	1
2. Keywords.....	1
3. Accomplishments.....	1
4. Impact.....	8
5. Changes/Problems.....	9
6. Products.....	11
7. Participants & Other Collaborating Organizations.....	11
8. Special Reporting Requirements.....	15
9. Appendices.....	15

1. INTRODUCTION

A significant number of women with high-grade serous ovarian cancer (HGSC) are intrinsically refractory to standard platinum-based treatment. We have previously shown that amplification of the cyclin E1 gene (*CCNE1*) in HGSC is associated with primary chemoresistance and poor clinical outcome. Cyclin E1 complexes with CDK2 to regulate cell cycle G1/S transition. Deregulation of cell cycle control is thought to be a prerequisite for tumour development and several studies have shown accelerated entry into S phase due to constitutive expression of *CCNE1*. Cyclin E1 is also able to induce chromosome instability by inappropriate initiation of DNA replication and centrosome duplication. We have demonstrated that *CCNE1*-amplified tumour cells are highly sensitive to knockdown of *CCNE1* or *CDK2*. Our current goal is to further advance novel therapeutic approaches to targeting *CCNE1* amplification through the development and characterisation of genetically engineered mouse (GEM) models of *Ccne1*-amplified HGSC. We also aim to identify and characterise additional genetic events that enhance cyclin E1-mediated transformation in fallopian tube secretory epithelial cells (FTSECs), the likely cell of origin in HGSC, using a high-throughput CRISPR-mediated genome-wide loss of function (LOF) screen. Results generated from this study have significant potential for clinical translation in HGSC, as well as other solid tumours with high frequency of *CCNE1* amplification including gastric, breast, and esophageal cancer.

2. KEYWORDS

Cyclin E1, CCNE1, amplification, genomic instability, high-grade serous ovarian cancer (HGSC), chemoresistance, mouse models, fallopian tube, homologous recombination (HR)

3. ACCOMPLISHMENTS

(A) Major Goals of the Project

Site 1: Peter MacCallum Cancer Centre; Melbourne, VIC, Australia (Bowtell)

Site 2: University of Pennsylvania; Philadelphia, PA, USA (Drapkin)

Site 3: Dana-Farber Cancer Institute; Boston, MA, USA (Berhoukim)

SPECIFIC AIM 1: GENERATE A TRANSGENIC MOUSE MODEL	Timeline (Months)	Site 1 (PI)	Site 2 (Co-PI)	Site 3 (Co-PI)	% Completed
Major Task 1: Generate transgenic <i>CAG-LSL-Ccne1</i> mice					
Subtask 1: Generate transgenes using the CMV early enhancer/chicken beta-actin (CAG) promoter, followed by a <i>loxP-STOP-loxP</i> cassette to provide conditional expression of full-length and low molecular weight forms of mouse <i>Ccne1</i>	1-3	*			100%

Subtask 2: Rosa26 <i>knock-in</i> - CAG promoter-driven, full length or LMW <i>Ccne1</i> cDNA will be knocked into the ROSA26 locus by homologous recombination	3-6	*			100%
Subtask 3: Southern Blot analysis to determine precise integration via homologous recombination in mouse ES cells. Blastocyst injection of targeted ES into sterile mouse embryos to generate a founder line. <i>*Outsourced to Ozgene</i>	6-12	*			67%
Major Task 2: Generate compound mutant mice by intercross and induce tumors	Months				
Subtask 1: Submit documents for local IRB and Animal Ethics review. <ul style="list-style-type: none"> Submission of institution approved animal protocols and related material for DoD's ACURO approval. Receive ACURO approval before initiating animal experiments. 	1-6	x	x		100%
Subtask 2: Interbreed breed CAG-LSL- <i>Ccne1</i> founding mice to expand the colony and obtain homozygous stock. <ul style="list-style-type: none"> Evaluate observed genotype ratios of animals generated for evidence of intrauterine or perinatal mortality and survey tissues from neonatal and adult mice histologically for normal development 	12-18	x			35%
Subtask 3: Intercross to Pax8 Cre-deletor mice, also carrying <i>Tp53</i> (R270H) and <i>Pten</i> ^{-/-} alleles. Confirm genotype.	15-18	x			0%
Subtask 4: Ship compound <i>CAG-LSL-Ccne1</i> , <i>Ccne1</i> ; <i>Tp53</i> ; Cre deletor, and <i>Ccne1</i> ; <i>Tp53</i> ; <i>Pten</i> ; Cre deletor mice to Drapkin lab and establish stock for investigation of early lesion studies	18-24	x	x		0%
Subtask 5: Administration of doxycycline (0.2mg/ml ad libitum) in the drinking water to induce expression of cyclinE1, mutant <i>Tp53</i> , and <i>Pten</i> deletion <ul style="list-style-type: none"> Monitor animals by ultrasound, body weight, and 	18-24	x			0%

physical examination on a weekly basis for tumor development. • Ship tumor blocks to Drapkin lab.					
Milestone #1: Established the Ccne1 model					
Major Task 3: Pathologically and genomically characterize tumours. Compare tumors in different transgenic and mutant backgrounds	Months				
Subtask 1: Evaluate Pax8, Stathmin-1, Ccne1, Ki-67, Pten and Tp53 expression compared to controls using immunohistochemistry	24-30		x		0%
Subtask 2: Evaluate DNA copy number by low coverage (~6X) whole genome sequencing (WGS). Compare copy number profiles to human HGSC with CCNE1 amplification to identify syntenic regions of gain or loss	24-36	x			0%
Subtask 3: Characterize the timing and penetrance of tumor development and investigate early lesions	24-36	x	x		0%
Milestone #2: Characterized tumours and co-authored manuscript.					
SPECIFIC AIM 2: INTERSECT FUNCTIONAL STUDIES IN FTSECS AND PAN-CANCER TUMOR GENOMIC DATA TO IDENTIFY GENES THAT COOPERATE WITH CCNE1 IN THE TRANSFORMATION OF FTSEC TO GUIDE THE DEVELOPMENT OF COMPOUND CYCLINE1 GEM MODELS.	Timeline	Site 1 (PI)	Site 2 (Co-PI)	Site 3 (Co-PI)	% Completed
Major Task 4: shRNA screen of FTSEC over expressing CCNE1 performed in Victorian Centre for Functional Genomics (VCFG)					
Subtask 1: Transduce cells at an MOI of ~ 0.3. Select cells by puromycin sensitivity and grow in soft agar. Isolate all the organoids, extract genomic DNA and perform next generation sequencing to identify shRNAs that are statistically abundant and potential drivers of the phenotype.	6-18	x			10%
Subtask 2: Utilise the VCFG bioinformatics pipeline for analysis of the sequencing data.	18-24	x			0%

Subtask 3: Orthogonal validation using CRISPR-mediated gene silencing	18-24	x			0%
<i>Milestone #3: Genes required in vitro for CCNE1-dependent FTSEC transformation and tumour cell survival identified</i>					
Major Task 5: Analyse shRNA and cDNA screen findings against pan-cancer data					
Subtask 1: Filter hits from the shRNA and cDNA screens using TCGA and ICGC pan-cancer data.	18-30			x	0%
<i>Milestone #4: In vitro screen observations supported by genomic data from human cancers</i>					

(B) Accomplishments Under These Goals

a. Major Activities

We primarily focused on the generation of transgenic *CAG-LSL-Ccne1* mice (Major Task 1) during the reporting period.

b. Specific Objectives

In order to complete the generation of transgenic *CAG-LSL-Ccne1* mice we had the following objectives:

- Identify a suitable promoter to drive *Ccne1* transgene expression in mice
- Design a vector for homology-mediated targeting of *Ccne1* to the *Rosa26* locus
- Perform successful ESC targeting and blastocyst injection to generate transgenic animals

c. Significant Results or Key Outcomes

Testing of the CAG & UBC promoters in FTSECs. As stated in the proposal, we planned to use the synthetic CAG promoter to drive expression of *Ccne1* at the *Rosa26* locus as it expressed across a wide range of mouse tissues and has been used extensively for transgene expression in mice. We also wanted to compare it to the human UBC promoter, which is also commonly used for transgene expression. As neither promoter had been targeted to FTSEC, we could not predict which would be more appropriate for our studies. Therefore as an initial guide, we generated GFP constructs with each promoter and transfected these into FTSEC lines to monitor expression. Under optimal transfection conditions, we found that the CAG promoter was able to drive strong GFP expression in 35.9% of transfected FTSECs versus the UBC promoter, which only stimulated GFP expression in 12.7% of cells (Figure 1). These results indicated that the CAG promoter was the most suitable for expression of *Ccne1* in mice. Subsequently, Ozgene approached us about pursuing the comparison of the CAG and UBC promoters *in vivo*, and agreed to generate an additional *UBC-LSL-Ccne1* mouse strain for direct comparison with the *CAG-LSL-Ccne1* at no cost.

Successful generation of UBC-LSL-CCNE1 and CAG-LSL-LMW_Ccne1 transgenic mice.

Generation of the *Ccne1* transgenic mice was outsourced to Ozgene. Targeting vectors (Figure 2) were designed and produced to our specifications and included: the CAG or UBC promoter, a LoxP-STOP-LoxP (LSL) cassette, a neomycin selectable marker, and the coding sequence (cDNA) for either full-length or a low molecular weight (LMW) isoform of *Ccne1* (Appendix A). Ozgene was able to successfully integrate *UBC-LSL-Ccne1* and *CAG-LSL-LMW_Ccne1* into the *Rosa26* locus in ES cells and generate homozygous stocks of mice (Figure 3 & Figure 4). These mice were subsequently shipped to the Peter MacCallum Animal Facility, where we have been able to successfully genotype, expand, and maintain colonies (Figure 5). Furthermore, to facilitate the generation of compound mutant mice, both the Bowtell and Drapkin laboratories have submitted animal ethics protocols and received approval from their respective Animal Ethics Committees (Appendix B & Appendix C).

Multi-copy CAG-LSL-Ccne1 transgenic mice. Ozgene also reported successful generation of *CAG-LSL-Ccne1* targeted ES cells and subsequent germline transmission in mice. However, in the course of further characterisation of the mice it became apparent that there are multiple integrants in the locus, perhaps up to 10 copies. We have obtained these mice and continue to characterise them while Ozgene has returned to generating single copy precise intergrants of the *CAG-LSL-Ccne1* transgene. It may be that the additional copies will provide enhanced expression that is serendipitously useful or be transcriptionally leaky and not appropriate for our studies. Will characterise the single and multiple copy animals until we have a clear outcome.

Optimization of soft agar growth conditions for FTSECs for the genome-wide screen (Aim 2). We have optimized conditions for soft agar growth of FTSECs in 6-well tissue culture dishes to facilitate positive selection in the genome-wide loss-of-function screen. We are currently working on establishing FTSECs with stably expression of Cas9.

FIGURES:

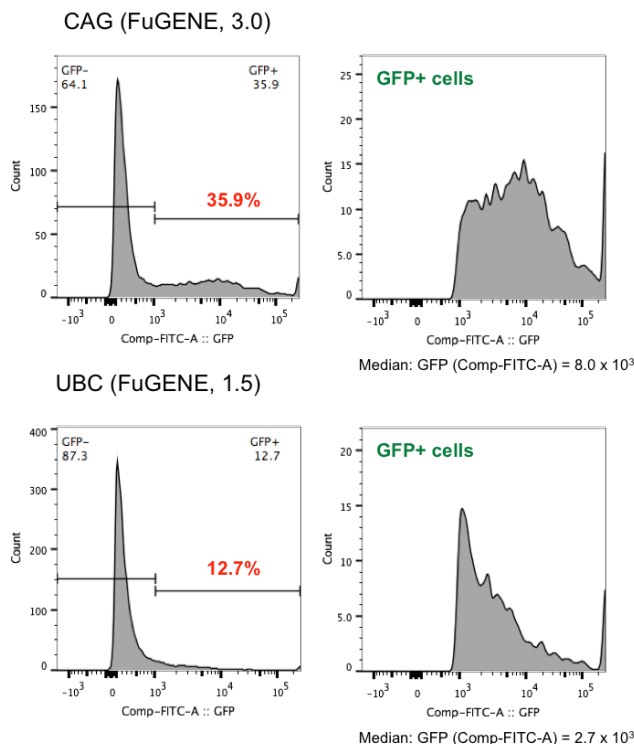


Figure 1. CAG and UBC driven expression of GFP in FTSECs. FACS analysis for GFP expression in FTSECs optimally transfected with vectors containing either the CAG or UBC promoter and a GFP reporter protein.

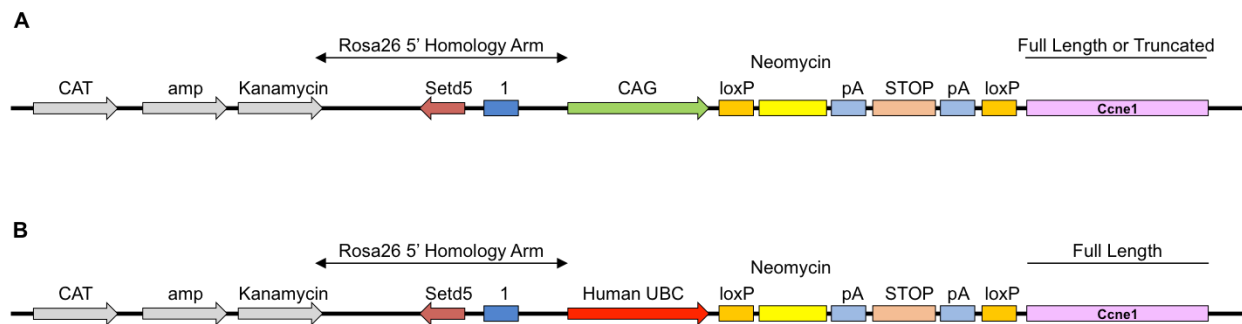


Figure 2. Targeting vectors used to facilitate insertion of *Ccne1* at the Rosa26 locus. (A) The CAG promoter vector used to generate mice expressing full length or truncated *Ccne1*. (B) The UBC promoter used to generate mice expressing full length *Ccne1*. Note the presence of a loxP-STOP-loxP cassette facilitating conditional expression of *Ccne1* via Cre recombinase.

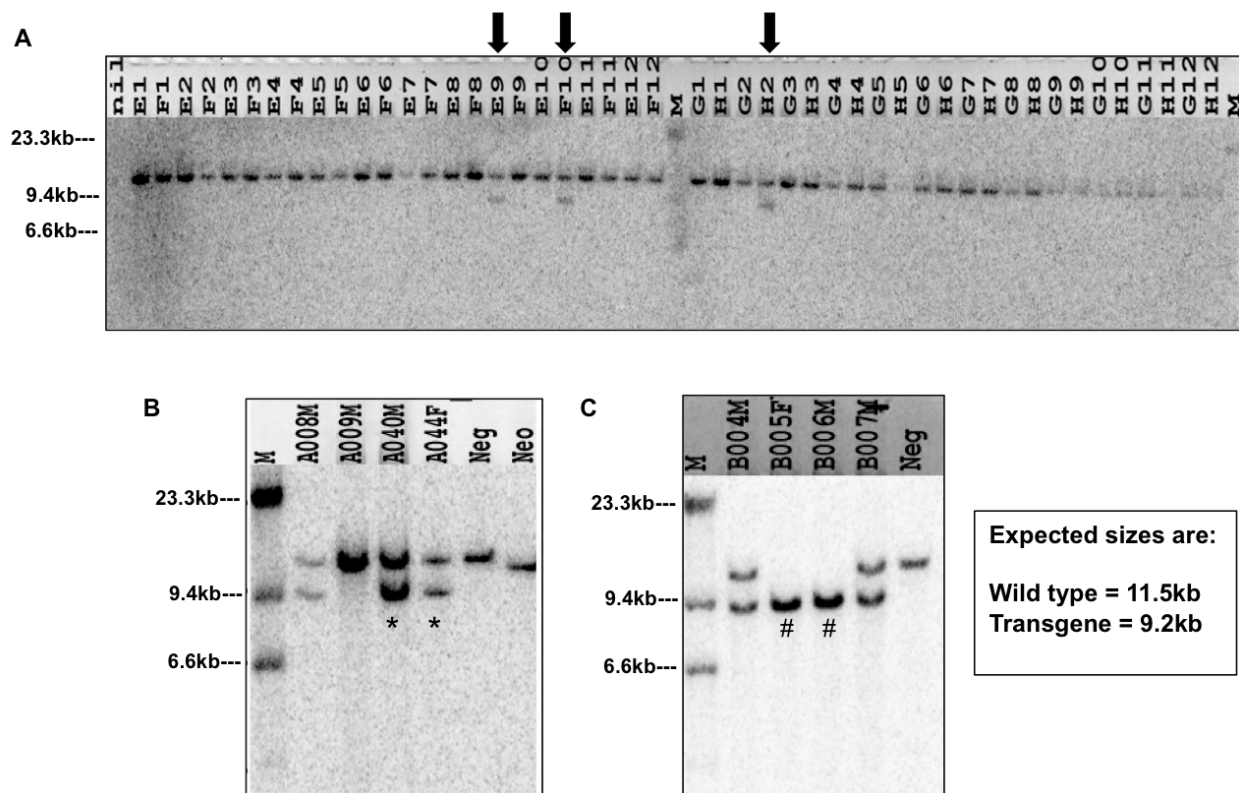


Figure 3. Successful ES cell targeting and germline transmission of *CAG-LSL-LMW_Ccne1*. South blot screening of: (A) targeted ES cells identified positive clones as indicated by the black arrows; (B) chimera mice identified successful germline transmission as indicated by *; (C) heterozygous founder mating identified homozygous offspring as indicated by #.

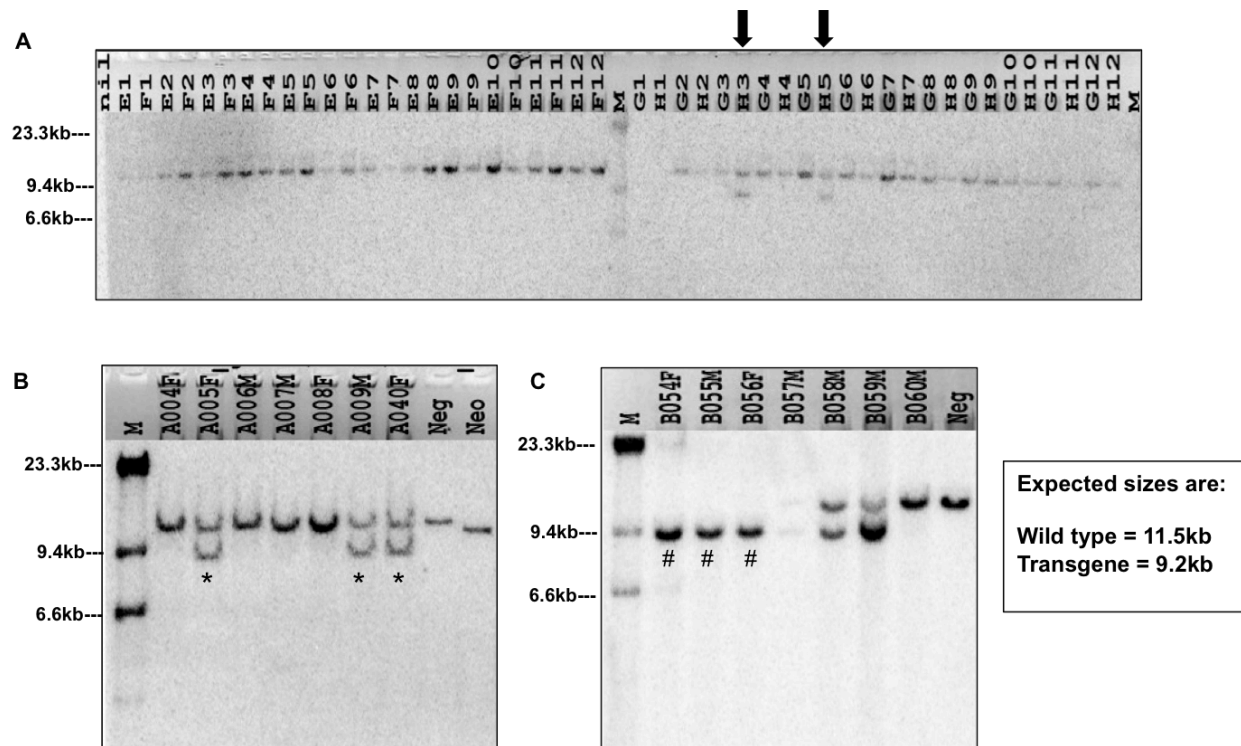


Figure 4. Successful ES cell targeting and germline transmission of *UBC-LSL-Ccne1*. South blot screening of: (A) targeted ES cells identified positive clones as indicated by the black arrows; (B) chimera mice identified successful germline transmission as indicated by *; (C) heterozygous founder mating identified homozygous offspring as indicated by #.

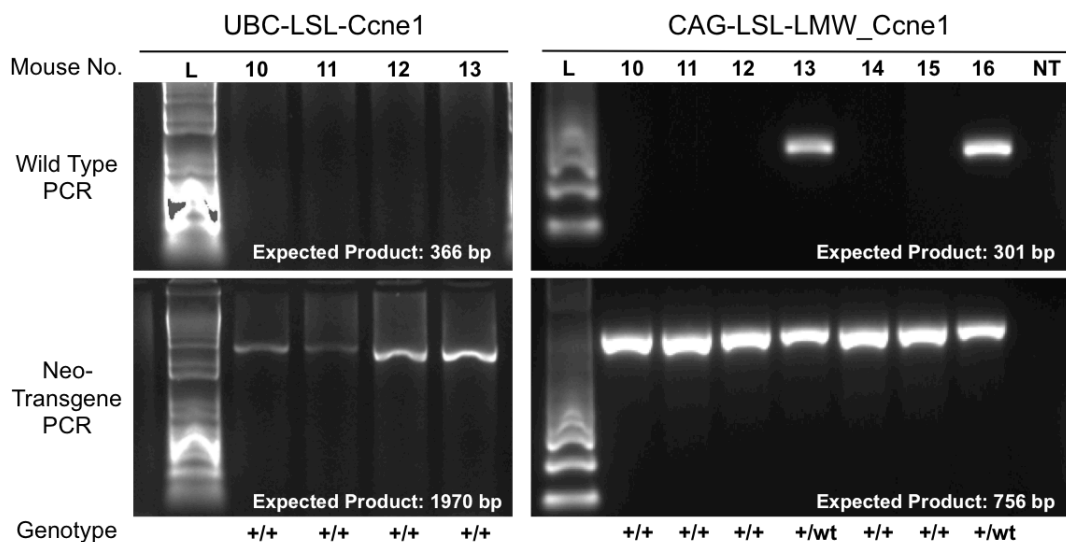


Figure 5. Genotyping PCR. Successful breeding of homozygous *UBC-LSL-Ccne1* and *CAG-LSL-LMW-Ccne1* mice at the Peter MacCallum Animal Facility.

d. Other Achievements

We identified AKT inhibition as a potential therapeutic combination with the CDK2 inhibitor dinaciclib in *CCNE1* amplified HGSC cell lines. The results of this study are shown in the attached manuscript (Appendix D: Au-Yeung et al, Clinical Cancer Research, 2016, in press) and are briefly described below.

We showed that CDK2 is a highly selective target for *CCNE1* amplified high-grade serous ovarian cancer (HGSC), using siRNA and conditional shRNA systems *in vitro* and *in vivo*. However, we found that dinaciclib, a small molecule CDK inhibitor, did not trigger amplicon dependent sensitivity in a panel of HGSC cell lines. This is likely due to the non-specific nature of small molecule CDK inhibitors such as dinaciclib, which although it is a potent inhibitor of CDK2, also inhibits CDK1, 5, 9 and 12. In order to improve on the efficacy of dinaciclib, we conducted a high throughput compound screen of over 4000 known drugs and targeted agents to identify selective synergistic combinations. We also aimed to identify combinations that may overcome drug resistance by including a CDK-inhibitor resistant cell line previously derived from a sensitive, *CCNE1*-amplified cell line. We obtained a number of hits, and focused particularly on a combination of dinaciclib and AKT inhibitors that were synergistic in *CCNE1*-amplified HGSC. We orthogonally validated the interaction between *CCNE1* and *AKT*, both in genomic data from TCGA and functionally in fallopian tube secretory cells, the target of HGSC transformation. In summary, our findings support CDK2 as a specific target for *CCNE1* amplified HGSC, and identify a combination of dinaciclib and AKT inhibitors that may inform the design of a rational clinical trial targeting an important subset of HGSC.

(C) Opportunities for Training and Professional Development

Nothing to Report

(D) Dissemination of Results to Communities of Interest

Nothing to Report

(E) Plans for Next Reporting Period to Accomplish the Goals

Our overall goal is to develop a GEM model of *Ccne1*-amplified HGSC to better understand disease initiation and to facilitate the development of novel therapeutic strategies. To this end, over the next year, we will finish generating the *CAG-LSL-Ccne1* mouse strain and begin generating compound mutant mice by intercrossing the *Ccne1* mouse strains with *Pax8-TetO-Cre-Tp53* mice (as outlined in the proposal). Once the compound mutant mice are established, we plan to induce *Ccne1* expression and *Tp53* deletion via doxycycline administration and systematically monitor mice for tumour development. The Drapkin and Bowtell laboratories will pathologically and genomically characterize any tumours that develop, respectively. Finally, we will finish optimization of conditions (transduction and soft agar growth) and carry out the high-throughput CRISPR-mediated gene knockout screen in FTSECs. Results from the screen will identify tumor suppressor genes that cooperate with *CCNE1* in the transformation of FTSECs, and guide the selection of alternative genes to develop additional compound GEM models using the *CAG-LSL-Ccne1-Tp53* strains.

4. IMPACT

(A) Impact on the Development of the Principal Discipline(s) of the Project

Nothing to Report

(B) Impact on Other Disciplines

Nothing to Report

(C) Impact on Technology Transfer

Nothing to Report

(D) Impact on Society Beyond Science and Technology

Nothing to Report

5. CHANGES/PROBLEMS

(A) Changes in Approach and Reason for Change

Selection of a CRISPR-Cas9 approach for the loss-of-function screen (Aim 2.1). At the time of the proposal submission, CRISPR-Cas9 was just emerging as a powerful tool for manipulating genomes, including genome-wide loss-of-function (LOF) screens. We had planned to perform an shRNA positive selection screen to identify tumour suppressors that cooperate with *CCNE1* in the transformation of FTSECs, however we indicated that we were open to adopting a CRISPR-Cas9 approach as the methodology evolved. Recent publications have compared CRISPR-Cas9 to shRNA-based genome-wide LOF screens in human cancer cell lines and found CRISPR-Cas9 to be superior in identifying essential/lethal genes, which suggests that complete gene inactivation may be necessary to identify cellular dependencies (Munoz et al *Cancer Discovery* 2016; Aguirre et al *Cancer Discovery* 2016). Therefore, we have elected to use a CRISPR-Cas9 approach in our genome-wide LOF screen. This screen will be performed in the Victorian Centre for Functional Genomics (VCFG), located at the Peter MacCallum Cancer Centre as previously described in the proposal. The overall workflow for the screen will remain as described for the shRNA screen including soft agar growth selection and next generation sequencing to identify guide RNAs (gRNAs) that are statistically abundant and potential drivers of the phenotype. The VCFG have obtained, expanded, and sequenced the human CRISPR Brunello lentiviral pooled library (two-vector system), which was designed using optimized metrics and consists of four gRNAs per gene for a total of 76,441 gRNAs (Doench et al *Nat Biotechnol.* 2016). The switch to a CRISPR-based approach results in a slight delay as the VCFG have obtained the libraries and developed virus. During this time we have optimized conditions for soft agar growth of FTSECs, and are currently generating the required FTSEC lines stably expressing Cas9. Since any intercross into mice of additional mutant alleles revealed by the CRISPR screen requires prior characterisation of the GEM mouse model, the delay in initiating the screen will not impact on the overall timeline for the study.

Deprioritization of *Pten* deletion from the breeding scheme. As stated in the proposal Aim 2.2, we plan to filter hits identified in the CRISPR-mediated LOF screen (and other previously performed cyclin E1 gain-of-function and LOF screens) to identify the most relevant genes to assess in mice. As an initial filter, we utilized pan-cancer data from TCGA and identified genes that are frequently altered by somatic genetic events (amplification or deletion), and for which these events are positively correlated with *CCNE1* amplification, suggesting cooperativity. Our preliminary results indicate that *PTEN* deletion does not significantly co-occur with *CCNE1*

amplification in human cancers (Table 1). Although loss of Pten significantly reduced tumour latency in PI Drapkin's *BRCA1/2* model we have deprioritized the crossing of *CAG-LSL-Ccne1-Tp53* mice with *Pten*^{-/-} mice, as it would not reflect the biology of human HGSC. It is quite possible that the combination of *Ccne1* over expression and *Tp53* deletion will be sufficient for generating HGSC in the mouse. However, in parallel, we will also consider other mutations/deletions identified in our loss-of-function screen, which may be introduced into the *CAG-LSL-Ccne1-Tp53* GEM model to enhance *in vivo* transformation.

Rank	Peak	Correlative p-value	Gene(s)
1	del_22q11.1	0.0051	<i>IL17RA, POTECH, CCT8L2, XKR3, CECR7</i>
2	amp_ERBB2	0.0212	<i>ERBB2</i>
3	del_KMT2C	0.0236	<i>KMT2C</i>
4	amp_(MCL1)	0.0254	<i>ENSA, GOLPH3L</i>
5	amp_17q11.2	0.0275	<i>FLOT2, ERAL2, FAM222B, PHF12, SEZ6</i>
106	del_PTEN	0.9966	<i>PTEN</i>

Table 1. Genetic Alterations That Correlate with CCNE1 Amplification. GISTIC peaks (from the "2015-06-01 stddata__2015_04_02 arm-level peel-off" analysis at <http://www.broadinstitute.org/tcga>) with the p-values for correlation of the peak event with amplification of *CCNE1* in the pan-cancer TCGA dataset.

(B) Actual or Anticipated Problems or Delays and Actions or Plans to Resolve Them

Relocation of Peter MacCallum Cancer Centre. In June 2016, Peter MacCallum Cancer Centre relocated to the new Victorian Comprehensive Cancer Centre building in the Parkville precinct of Melbourne. This relocation resulted in the Peter MacCallum Animal Facility being unable to accept external mouse importations from approximately April to August 2016, which impacted the shipment of the *Ccne1* mouse strains from Ozgene. To keep the project on track, we contracted Ozgene to interbreed the *UBC-LSL-Ccne1* and the *CAG-LSL-LMW_Ccne1* founding mice to expand the colonies and obtain homozygous stocks. We received homozygous breeding pairs for both strains in mid-August 2016, and have successfully continued to expand these colonies.

Relocation of the Drapkin Laboratory. During Year 1 of the grant, PI Drapkin accepted a new position at the University of Pennsylvania that required the relocation of his laboratory to Philadelphia, Pennsylvania. Due to the necessary shipment and reestablishment of the Drapkin laboratory mouse strains at the new animal facility, there has been a delay in receiving the *Pax8-TetOCre-Tp53* mice required for interbreeding with the *Ccne1* mice. We anticipate shipment of three breeding pairs of *Pax8-TetOCre-Tp53* mice to Peter MacCallum Cancer Centre in February 2017. Additionally, we have identified a laboratory in Australia that has an alternative *Pax8-TetOCre* mouse strain that can be imported to Peter MacCallum Cancer Centre if the delay in shipment from the Drapkin laboratory is longer than expected.

Multiple Integrations of Ccne1 in CAG-LSL-Ccne1 Mice. In May 2016, we were informed by Ozgene that in the process of reconfirming integration of *Ccne1* in the germline offspring, they identified that the *CAG-LSL-Ccne1* mice had multiple integrations of the vector at the *Rosa26* locus. Unfortunately, frozen stocks of targeted *CAG-LSL-Ccne1* mouse ES cells were not viable, and Ozgene had to begin *de novo* derivation of the strain. As of this report, Ozgene has achieved successful single integration and germline transmission of *CAG-LSL-Ccne1*, with heterozygous mice anticipated for shipment in late-January 2017. Although it will be important to have strain with single integration of *Ccne1*, we believe that *CAG-LSL-Ccne1* mice with multiple integrations (*CAG-LSL-Ccne1_multi*) may also prove useful given that patients with HGSC can

have more than eight copies of *CCNE1*. Therefore, we have elected to maintain the *CAG-LSL-Ccne1_multi* mouse strain (provided by Ozgene at no cost) and characterize it in parallel with the other established mouse strains as an interim measure.

(C) Changes That Had a Significant Impact on Expenditures

Nothing to Report

(D) Significant Changes in Use or Care of Human Subjects, Vertebrate Animals, Biohazards, and/or Select Agents

In regard to animal ethics protocol titled “Genetically Engineered Mouse Models of Ovarian Cancer”, IACUC protocol E561, we have submitted and received approval from the Peter MacCallum Animal Experimentation Ethics Committee to add an additional investigator (Dr. Jessica Beach). The amendment was approved 21 April 2016 and these changes were reported via email to ACURO on 1 September 2016.

6. PRODUCTS

(A) Journal Publications

Au-Yeung G, Lang F, Mitchell C, Jarman KE, Lackovic K, Aziz D, Cullinane C, Pearson RB, Mileschkin L, Rischin D, Karst AM, Drapkin R, Etemadmoghadam D, Bowtell DD. Selective targeting of Cyclin E1 amplified high grade serous ovarian cancer by cyclin-dependent kinase 2 and AKT inhibition. *Clinical Cancer Research*, 2016. Advanced online publication. doi: 10.1158/1078-0432.CCR-16-0620.

Acknowledgement of federal support: Yes

(B) Other Products—Research Material

We have generated two of three planned GEM strains with mouse cyclin E1 (*Ccne1*; full length or truncated) expressed under the control of the *CAG* or human *UBC* promoter at the *Rosa26* locus. Furthermore, our targeting construct contained a *loxP*-STOP-*loxP* cassette allowing for tissue-specific, *Cre*-mediated excision of the cassette and conditional expression of *Ccne1*. These mouse strains may be beneficial in the generation of GEM models of other CCNE1-amplified cancers, such as gastric cancer.

Mouse Strain	Status
C57Bl6-Gt(ROSA)26Sor ^{tm1(LSL-CAG-Ccne1)Ozg}	Anticipated in February 2017
C57Bl6-Gt(ROSA)26Sor ^{tm1(LSL-UBC-Ccne1)Ozg}	Established
C57Bl6-Gt(ROSA)26Sor ^{tm1(LSL-CAG-LMWCcne1)Ozg}	Established

7. PARTICIPANTS

(A) Individuals who have worked on this project

The following individuals have contributed to the project:

Name:	David Bowtell
Project Role:	PI
Nearest Person Month Worked:	1
Contribution to Project:	No Change

Name:	Ronny Drapkin
Project Role:	Co-PI
Nearest Person Month Worked:	1
Contribution to Project:	No Change

Name:	Rameen Berhoukim
Project Role:	Co-PI
Nearest Person Month Worked:	1
Contribution to Project:	No Change

Dr. Dariush Etemadmoghdam was named under other personnel as the postdoctoral fellow on this project at Peter MacCallum Cancer Centre, however Dr. Etemadmoghdam has taken on a new role that means he no longer has the required time to commit to the project. In his place, we plan to deploy Dr. Jessica Beach, who also has the required and appropriate experience to be the postdoctoral fellow on this project (see below). As this role is not due to commence until year 2 of this project (1 October 2016) we anticipate that this personnel change will have no impact on the progress of the project or the budget.

Name:	Jessica A. Beach
Project Role:	Postdoctoral Fellow
Research Identifier:	orcid.org/0000-0001-9995-9892
Nearest Person Month Worked:	6 (anticipated each year)
Contribution to Project:	Dr. Beach will coordinate all aspects of the study being performed at Peter MacCallum Cancer Centre including animal breeding, animal model characterisation, and the high-throughput gene knockout screen.

(B) Changes in Active Other Support of the PI or Key Personnel

David Bowtell (PI)

Pending to Active Research Support:

APP1092856 (Bowtell)	2016 – 2020
NHMRC Program Grant	
Improving Outcomes for Women with Epithelial Ovarian Cancer	
Role: Principal Investigator (40% effort)	
Awarded: \$374,632 AUD (annual direct costs)	

OC150563 (Pike/Pearce)	2016 – 2019
US Department of Defense Ovarian Cancer Research Program	
Multidisciplinary Ovarian Cancer Outcomes Group (MOCOG)	
Role: Key Personnel (5% effort Year 1, 2, 3; 4% effort Year 4)	
Awarded: \$216,418 (direct costs)	

APP 14/TPG/1-15 (deFazio) 2015 – 2019
Cancer Institute NSW Translational Program Grant
INOVATe - Individualised Ovarian Cancer Treatment Through Integration of Genomic Pathology
into Multidisciplinary Care
Role: Chief Investigator E (5% effort)

Active to Completed Research Support:

APP1044447 (Bowtell) 2013 – 2015
NHMRC Project Grant
Novel Therapeutic Approaches to Ovarian Clear Cell Cancer
Role: Chief Investigator A

Ronny Drapkin (Co-PI)

Pending to Active Research Support:

No Number (Drapkin) 2013 – 2017
Tina Brozman Foundation
Ex vivo culture of fallopian tube epithelium for proteomic detection of biomarkers in ovarian
cancer
Role: Principal Investigator (5% effort)
Awarded: \$45,455 (annual direct costs)

No Number (Drapkin) 2016 – 2016
Tina Brozman Foundation
Tina Brozman Ovarian Cancer Consortium (TBOCC)
Role: Principal Investigator (5% effort)
Awarded: \$33,174 (annual direct costs)

Active to Completed Research Support:

R21 CA156021 (Drapkin) 2013 – 2015
NIH/NCI
Elafin as a biomarker in serous ovarian cancers and basal-like breast tumors
Role: Principal Investigator (15% effort)
Awarded: \$57,925 (annual direct costs)

Rameen Berhoukim (Co-PI)

Pending to Active Research Support:

5 R01 CA188228-02 (Beroukhim, Ligon) 2015 – 2020
NIH Project Grant
Genetic Evolution of Glioblastoma During Radiation and Temozolomide Therapy
Role: Principal Investigator (20% effort)
Awarded: \$448,351 (annual direct cost)

No Number (Beroukhim) 2015 – 2016
Ian's Friend's Foundation

Identifying Therapeutic Targets of MYB-QK1 Fusions in Pediatric Low-Grade Glioma

Role: Key Personnel (1% effort)

Awarded: \$100,000 (direct costs)

No Number (Beroukhim)

2016 – 2016

Cure Starts Now

Characterizing resistance mechanisms to radiation and adjuvant therapy in DIPG

Role: Key Personnel (1% effort)

Awarded: \$90,909 (direct costs)

Footridge Award (Lindquist, Santagata, Beroukhim)

2016 – 2017

KI-DF/HCC Bridge Program

Modulating the heat-shock machinery to limit genetic heterogeneity and evolution of highly malignant cancers

Role: Key Personnel (2% effort)

Awarded: \$41,288 (Beroukhim portion, direct costs)

Innovation Grant (Beroukhim)

2015 – 2017

Alex's Lemonade Stand Foundation

Characterizing resistance mechanisms to BET-bromodomain inhibition of MYC-amplified medulloblastoma

Role: Principal Investigator (12.5% effort)

Awarded: \$125,000 (annual direct cost)

No Number (Beroukhim)

2016 – 2016

Broad Institute SPARC (Scientific Projects to Accelerate Research & Collaboration)

EvoSeq: A molecular time machine to study evolution

Role: Key Personnel (2% effort)

Awarded: \$185,000

No Number (Beroukhim)

2016 – 2017

St. Baldrick's Foundation

Intratumoral heterogeneity of resistance drivers in DIPG

Role: Key Personnel (1% effort)

Awarded: \$100,000 (direct costs)

No Number (Beroukhim)

2016 – 2018

Pediatric Brain Tumor Foundation

BRD4 as a therapeutic target in medulloblastoma

Role: Principal Investigator (5% effort)

Awarded \$100,836 (annual direct costs)

U24 CA210978-01 (Beroukhim, Cherniack)

2016 – 2021

NIH Resource-Related Research Projects

Center for the comprehensive analysis of somatic copy-number alterations in cancer

Role: Principal Investigator (20% effort)

Awarded: \$412,500 (annual direct costs)

(C) Other Partner Organizations

Nothing to Report

8. SPECIAL REPORTING REQUIREMENTS

None

9. APPENDIX

Appendix A: *Ccne1* Sequences Used for Targeting

Appendix B: E561 Animal Ethics Approval, Peter MacCallum Cancer Centre (Bowtell)

Appendix C: 806138 Animal Ethics Approval, University of Pennsylvania (Drapkin)

Appendix D: Journal article in press, Au-Yeung et al. *Clinical Cancer Research* 2016

APPENDIX A: *Ccne1* Sequences Used for Targeting

CAG-LSL-*Ccne1* (1615_Truman)

>Mouse_CCNE1_FullLength_CDS

ATGCCAAGGGAGAGAGACTCGACGGACCACAGCAACATGAAAGAAGAAGGTGGCTCCGACCTTTTCAGTCCGCTCCAG
AAAAAGGAAGGCAAATGTGGCCGTGTTTTTGCAGACCCAGATGAAGAAATTGCCAAGATTGACAAGACTGTGAAAA
GCGAGGATAGCAGTCAGCCCTGGGATGATAATTCAGCATGCGTGGACCCCTGCTCTTTTCATCCCCACCCCTAACAAA
GAAGAGGACAATGAGCTTGAATACCCAGGACTGCATTTTCAGCCTCGGAAAATCAGACCACCCAGAGCCTCCCCACT
TCCCGTCTTGAATTGGGGCAATAGAGAAGAGGTTTGGAGGATCATGTTAAACAAAGAAAAGACTTACCTGAGAGATG
AGCATTCTTCTGCAGCGTCATCCTCTCCTGCAGGCGAGGATGAGAGCAGTTCTTCTGGATTGGCTAATGGAGGTGTGC
GAAGTCTATAAGCTCCACAGAGAGACGTTCTACTTGGCACAGGACTTCTTTGATCGTTACATGGCATCACAAACATAA
TATCATAAAAAACACTTTTACAGCTTATTGGGATTTTCAGCCTTATTTATTGCTTCAAACTTGAGGAAATCTACCCTC
CAAAGTTGCACCAGTTTGCTTATGTTACAGATGGCGCTTGCTCCGGGGATGAAATTCTTACCATGGAATTGATGATG
ATGAAGGCCCTTAAGTGGCGTCTAAGCCCTCTGACCATTGTGTCTTGCTGAATGTCTATGTCCAAGTGGCCTATGT
CAACGACACGGGTGAGGTGCTGATGCCTCAGTACCCACAGCAGGTCTTCGTGCAGATCGCAGAGCTTCTAGACCTGT
GCGTCTCGGATGTTGGCTGCTTAGAATTTCTTATGGTGTCTCGCTGCTTCTGCTTTGTATCATTTCTCCTCACTG
GAGTTGATGCAGAAGGTCTCAGGTTATCAGTGGTGCGACATAGAGAAGTGTGTCAAATGGATGGTTCCGTTCCGCAT
GGTTATCCGGGAGATGGGAAGTTCCAAGCTCAAGCACTTCCGGGGAGTCCCATGGAAGACTCCCAACATCCAGA
CCCACACCAACAGCTTGGATTTGCTGGACAAAGCCCAAGCAAAGAAAGCCATATTGTCAGAACAGAATAGGATTTCT
CCTCCTCCGAGTGTGGTCTGACACCCCCACCCAGCAGTAAGAAGCAGAGCAGCGAGCAGGAGACAGAATGA

>Mouse_CCNE1_FullLength_Protein

MPRERDSTDHNSMKEEGGSDLSVRSRKRKANVAVFLQDPDEEIAKIDKTVKSEDSSQPWDDNSACVDPCSFIPTPNK
EEDNELEYPRTAFOPRKIRPPRASPLPVLNWNREEVWRIMLNKEKTYLRDEHFLQRHPLLQARMRAVLLDWLMEVC
EVYKLHRETFYLAQDFFDRYMASQHNIIKTLLQLIGISALFIASKLEEIYPPKLHQFAYVTDGACSGDEILTMELMM
MKALKWRLSPLTIVSWLNVYVQVAYVNDTGEVLMPOYPQOVFVQIAELLDLCVLDVGCLEFPYGVLAASALYHFSSL
ELMQKVSQYQWCDIEKCVKWMVPFAMVIREMGSSKLKHFRGVPMEDSHNIQTHTNSLDLLDKAQAKKAILSEQNRIS
PPPSVVLTPPPSSKKQSSQSEETE

CAG-LSL-*Ccne1*-Truncated (1616_Enoch)

>Mouse_CCNE1_T1_Truncated_CDS

ATGGACCCAGATGAAGAAATTGCCAAGATTGACAAGACTGTGAAAAGCGAGGATAGCAGTCAGCCCTGGGATGATAA
TTCAGCATGCGTGGACCCCTGCTCTTTTCATCCCCACCCCTAACAAAGAAGAGGACAATGAGCTTGAATACCCAGGA
CTGCATTTTCAGCCTCGGAAAATCAGACCACCCAGAGCCTCCCCACTTCCCGTCTTGAATTGGGGCAATAGAGAAGAG
GTTTGGAGGATCATGTTAAACAAAGAAAAGACTTACCTGAGAGATGAGCACTTTCTGCAGCGTCATCCTCTCCTGCA
GGCAGGATGAGAGCAGTTCTTCTGGATTGGCTAATGGAGGTGTGCGAAGTCTATAAGCTCCACAGAGAGACGTTCT
ACTTGGCACAGGACTTCTTTGATCGTTACATGGCATCACAAACATAATATCATAAAAAACACTTTTACAGCTTATTGGG
ATTTTCAGCCTTATTTATTGCTTCAAACTTGAGGAAATCTACCCTCCAAAGTTGCACCAGTTTGCTTATGTTACAGA
TGGCGCTTGCTCCGGGGATGAAATTCTTACCATGGAATTGATGATGATGAAGGCCCTTAAGTGGCGTCTAAGCCCTC
TGACCATTGTGTCTTGCTGAATGTCTATGTCCAAGTGGCCTATGTCAACGACACGGGTGAGGTGCTGATGCCTCAG
TACCCACAGCAGGTCTTCGTGCAGATCGCAGAGCTTCTAGACCTGTGCGTCTCGGATGTTGGCTGCTTAGAATTTCC
TTATGGTGTCTCGCTGCTTCTGCTTTGTATCATTTCTCCTCACTGGAGTTGATGCAGAAGGTCTCAGGTTATCAGT
GGTGCACATAGAGAAGTGTGTCAAATGGATGGTTCCGTTCCGCATGGTTATCCGGGAGATGGGAAGTTCCAAGCTC
AAGCACTTCCGGGGAGTCCCATGGAAGACTCCCAACATCCAGACCCACACCAACAGCTTGGATTTGCTGGACAA
AGCCCAAGCAAAGAAAGCCATATTGTCAGAACAGAATAGGATTTCTCCTCCTCCGAGTGTGGTCTGACACCCCCAC
CCAGCAGTAAGAAGCAGAGCAGCGAGCAGGAGACAGAATGA

>Mouse_CCNE1_T1_Truncated_Protein

MDPDEEIAKIDKTVKSEDSSQPWDDNSACVDPCSFIPTPNKEEDNELEYPRTAFOPRKIRPPRASPLPVLNWNREE
VWRIMLNKEKTYLRDEHFLQRHPLLQARMRAVLLDWLMEVCEVYKLHRETFYLAQDFFDRYMASQHNIIKTLLQLIG
ISALFIASKLEEIYPPKLHQFAYVTDGACSGDEILTMELMMMALKWRLSPLTIVSWLNVYVQVAYVNDTGEVLMPO
YPQOVFVQIAELLDLCVLDVGCLEFPYGVLAASALYHFSSLELMQKVSQYQWCDIEKCVKWMVPFAMVIREMGSSKL
KHFRGVPMEDSHNIQTHTNSLDLLDKAQAKKAILSEQNRISPPPSVVLTPPPSSKKQSSQSEETE

APPENDIX B: E561 Animal Ethics Approval, Peter MacCallum Cancer Centre (Bowtell)



CANCER RESEARCH DIVISION

PETER MACCALLUM CANCER CENTRE ANIMAL EXPERIMENTATION ETHICS COMMITTEE (AEEC)	
Application For Approval To Use Animals In A Research Project	Date application received: 23/11/15 Resubmitted: 15/02/16

Office Use Only

Project Title AEEC Register Number

AEEC Permit Number


Genetically engineered mouse models of ovarian cancer

	E	5	6	1
--	---	---	---	---

DECLARATION BY AEEC CHAIRMAN

I certify that this project has been considered and approved by the Peter MacCallum Cancer Centre AEEC Chair on the 7th March 2016 and ratified by the full committee on the 26th May 2016.

The period of approval for this project is 07/03/16 to 06/03/19

AEEC Chairman Name:	A/Prof. Phillip Darcy
AEEC Chairman Signature:	
Date:	31/05/16

CONDITIONS OF APPROVAL

All matters pertaining to the conduct of the approved project are to be reported to the AEEC, which maintains oversight in accordance with licence conditions for the Licence SPPL078.

Any variation proposed to the project, and the reasons for that change, must be submitted to the AEEC for approval and must not be implemented until approval is granted.

A record of details of any animals used in the project must be retained.

The project should only be conducted in approved premises nominated on the Bureau of Animal Welfare Scientific Licence **SPPL078**.

The AEEC must also be notified in writing of;

- Any changes to approved investigators
- Any unexpected incidents or complications that result in deaths, euthanasia or pain and suffering for the animals used in the project. Details of the steps taken to deal with adverse incidents must be included in the notification.

OTHER CONDITIONS:

This approval is subject to the following special conditions:

APPENDIX C: 806138 Animal Ethics Approval, University of Pennsylvania (Drapkin)



IACUC Protocol Administration
<http://www.upenn.edu/animalwelfare>

Office of Animal Welfare
Science Center Building
3624 Market Street, Suite 301S
Philadelphia, PA 19104
Phone: 215-898-2615
Fax: 215-746-6308
Email: iacuc@pobox.upenn.edu

**UNIVERSITY OF PENNSYLVANIA
INSTITUTIONAL ANIMAL CARE AND USE COMMITTEE (IACUC)**
(Animal Welfare Assurance # A3079-01)

RONNY DRAPKIN
4333 - OB-Obstetrics and Gynecology
421 Curie Blvd
BRB II/III Suite 1215
Philadelphia, PA 19104-6160

10-Nov-2016

PRINCIPAL INVESTIGATOR : RONNY DRAPKIN
PROTOCOL TITLE : Using Genetically Engineered Mice for the Study High Grade Serous Ovarian Cancer
PROTOCOL # : 806138
3-YEAR APPROVAL PERIOD : 05-Nov-2016 – 05-Nov-2019

Dear DR. DRAPKIN:

The above referenced protocol was reviewed and approved by the Institutional Animal Care and Use Committee on **05-Nov-2016**. Protocols are valid for three years from the date of approval. However, please note that protocols with USDA-covered species will require annual continuing reviews. This study will be due for its next review on or before **05-Nov-2019**. Please log into the ARIES electronic protocol system (<https://aries.apps.upenn.edu/IaProtocol/jsp/fast2.do>) on a routine basis to check the status of your protocol, and be cognizant of reminder notifications that will be sent out when new submissions are required.

Please note that the principal investigator should contact ULAR to verify animal housing availability and to coordinate activities for any special animal study needs (including special housing) or equipment requirements if this was not done during the planning phases of the protocol. IACUC protocol approval DOES NOT guarantee the availability of required resources for animal work.

Please take note of the following information:

Personnel Training: It is the responsibility of the Principal Investigator to ensure that all persons have completed all necessary training prior to participating in the research described in this protocol.

Submissions: Please note that all future submissions related to this protocol must be submitted within ARIES. No paper submissions will be accepted.

Amendments: If you wish to change any aspect of this study, such as personnel, sponsors, hazardous materials, drugs, or procedures, please submit an Amendment to the protocol within ARIES. The new changes cannot be initiated until IACUC approval has been given.

Completion of Study: Please notify the Office of Animal Welfare once the research has been completed so the protocol can be terminated. This will prevent you from receiving unnecessary reminder notifications for renewal submissions.

If you have any questions, please contact our office as indicated above. Thank you for your cooperation with the Committee.

Sincerely,

A handwritten signature in black ink, appearing to read "Gregory R. Reinhard".

Gregory R. Reinhard, MBA, DVM, DACLAM
Director, Office of Animal Welfare

Digitally signed by Gregory R. Reinhard
Date: 2016.11.14 09:09:32 -05'00'

Selective Targeting of Cyclin E1-Amplified High-Grade Serous Ovarian Cancer by Cyclin-Dependent Kinase 2 and AKT Inhibition

George Au-Yeung^{1,2}, Franziska Lang¹, Walid J. Azar¹, Chris Mitchell¹, Kate E. Jarman³, Kurt Lackovic^{3,4}, Diar Aziz⁵, Carleen Cullinane^{1,6}, Richard B. Pearson^{1,2,7}, Linda Mileschkin^{2,8}, Danny Rischin^{2,8}, Alison M. Karst⁹, Ronny Drapkin¹⁰, Dariush Etemadmoghadam^{1,2,5}, and David D.L. Bowtell^{1,2,7,11}

Abstract

Purpose: Cyclin E1 (*CCNE1*) amplification is associated with primary treatment resistance and poor outcome in high-grade serous ovarian cancer (HGSC). Here, we explore approaches to target *CCNE1*-amplified cancers and potential strategies to overcome resistance to targeted agents.

Experimental Design: To examine dependency on *CDK2* in *CCNE1*-amplified HGSC, we utilized siRNA and conditional shRNA gene suppression, and chemical inhibition using dinaciclib, a small-molecule *CDK2* inhibitor. High-throughput compound screening was used to identify selective synergistic drug combinations, as well as combinations that may overcome drug resistance. An observed relationship between *CCNE1* and the AKT pathway was further explored in genomic data from primary tumors, and functional studies in fallopian tube secretory cells.

Results: We validate *CDK2* as a therapeutic target by demonstrating selective sensitivity to gene suppression. However, we found that dinaciclib did not trigger amplicon-dependent sensitivity in a panel of HGSC cell lines. A high-throughput compound screen identified synergistic combinations in *CCNE1*-amplified HGSC, including dinaciclib and AKT inhibitors. Analysis of genomic data from TCGA demonstrated coamplification of *CCNE1* and *AKT2*. Overexpression of Cyclin E1 and AKT isoforms, in addition to mutant *TP53*, imparted malignant characteristics in untransformed fallopian tube secretory cells, the dominant site of origin of HGSC.

Conclusions: These findings suggest a specific dependency of *CCNE1*-amplified tumors for AKT activity, and point to a novel combination of dinaciclib and AKT inhibitors that may selectively target patients with *CCNE1*-amplified HGSC. *Clin Cancer Res*; 1–15. ©2016 AACR.

Introduction

Targeted therapies have changed the management of many cancers types, resulting in significant improvements in clinical response rates and survival (1). However, the antiangiogenic mAb bevacizumab (2, 3) and the PARP inhibitor olaparib (4, 5) have entered care in high-grade serous ovarian cancer (HGSC) recently, the development of targeted therapy to this disease has been relatively slow.

HGSCs are characterized by ubiquitous *TP53* mutations, genomic instability, and widespread copy number alterations, with relatively infrequent somatic point mutations of driver genes (6, 7). Structural aberration also contributes to loss of tumor suppressors such as *RB1* and *NF1* by gene breakage (8). Defects in the homologous recombination repair (HR) pathway are present in approximately 50% of HGSCs, primarily associated with germline and somatic mutations in *BRCA1*, *BRCA2*, and associated proteins (7). HR deficiency imparts platinum sensitivity in HGSC, and provides the basis for the use of PARP inhibitors that target compensatory DNA repair pathways (4, 9). Of HGSC with intact HR, amplification of *CCNE1*, which encodes the cell-cycle regulator cyclin E1, is the best characterized driver. *CCNE1* amplification or gain occurs in 20% of all HGSC tumors and is associated with primary treatment resistance and reduced overall survival in HGSC (10, 11). Patients whose tumors have *CCNE1*

¹Division of Cancer Research, Peter MacCallum Cancer Centre, East Melbourne, Victoria, Australia. ²Sir Peter MacCallum Department of Medical Oncology, University of Melbourne, Parkville, Victoria, Australia. ³Walter and Eliza Hall Institute of Medical Research, Parkville, Victoria, Australia. ⁴Department of Medical Biology, University of Melbourne, Parkville, Victoria, Australia. ⁵Department of Pathology, University of Melbourne, Parkville, Victoria, Australia. ⁶Translational Research Program, Peter MacCallum Cancer Centre, East Melbourne, Victoria, Australia. ⁷Department of Biochemistry and Molecular Biology, University of Melbourne, Parkville, Victoria, Australia. ⁸Department of Medical Oncology, Peter MacCallum Cancer Centre, East Melbourne, Victoria, Australia. ⁹Department of Medical Oncology, Dana Farber Cancer Institute, Boston, Massachusetts. ¹⁰Division of Gynecologic Oncology, Department of Obstetrics and Gynecology, Penn Ovarian Cancer Research Center, University of Pennsylvania Perelman School of Medicine, Philadelphia, Pennsylvania. ¹¹Kinghorn Cancer Centre, Garvan Institute for Medical Research, Darlinghurst, New South Wales, Australia.

Note: Supplementary data for this article are available at Clinical Cancer Research Online (<http://clincancerres.aacrjournals.org/>).

D. Etemadmoghadam and D.D.L. Bowtell contributed equally to this article.

Corresponding Author: David D.L. Bowtell, Peter MacCallum Cancer Centre, Locked Bag 1, A's Beckett Street, Melbourne, Victoria 8006, Australia. Phone: 613-9656-1356; Fax: 613-9656-1414; E-mail: david.bowtell@petermac.org

doi: 10.1158/1078-0432.CCR-16-0620

©2016 American Association for Cancer Research.

Translational Relevance

High-grade serous ovarian cancer (HGSC) patients with Cyclin E1 (*CCNE1*) amplification represent a group with high unmet clinical need. Novel therapies are needed to improve outcomes in these patients, given that *CCNE1*-amplified tumors are unlikely to respond to chemotherapy or PARP inhibitors, and are associated with poor overall survival. Here, we validate *CDK2* as a selective target for *CCNE1*-amplified cell lines. We performed a high-throughput compound screen and identified a number of potential therapeutic combinations. We focused on dinaciclib and AKT inhibitors, and demonstrate selective and potent activity in *CCNE1*-amplified HGSC. We further show cooperation between *CCNE1* and *AKT*, both in genomic data from TCGA and functionally in fallopian tube secretory cells. This study demonstrates approaches to target an important subset of solid cancers, and for the first time provides evidence to support the design of a rational clinical trial that targets *CCNE1*-amplified HGSC.

amplification represent a group with unmet clinical need, as they are unlikely to benefit from PARP inhibitors by virtue of the mutual exclusivity of *CCNE1* amplification and *BRCA1/2* mutation (7, 12), and are less likely to respond to platinum agents. In recent preclinical studies, we have shown a dependency on *CDK2* (13) and HR activity (12) in *CCNE1*-amplified cell lines. Although targeted agents have been effective in the clinical setting across many cancers, the emergence of acquired resistance is common (14). Indeed, we reported *in vitro* resistance to *CDK2* inhibitors through selection of a polyploid population in the *CCNE1*-amplified cell line OVCAR3 (13). Rational drug combinations are a potential strategy to prevent resistance (15), and may also facilitate improvements in the therapeutic window by reducing the doses of drugs required to achieve efficacy, resulting in fewer side effects (16). We therefore used a high-throughput drug screen to identify drug combinations that synergize with the *CDK2* inhibitor dinaciclib (17) to selectively target *CCNE1*-amplified HGSC, and to overcome resistance in a cell line that has acquired resistance to *CDK* inhibitors *in vitro* (13). We identified several synergistic combinations, including dinaciclib and AKT inhibitors, and found that that this synergy extended more generally to *CCNE1*-amplified HGSC cell lines. Our results suggest targeting *CDK2* and the AKT pathway may be an important approach to the clinical management of *CCNE1*-amplified HGSC.

Materials and Methods

Ethics statement

All animal experiments were approved by the Peter MacCallum Cancer Centre Animal Experimentation Ethics Committee and conducted in accordance with the National Health and Medical Research Council Australian Code of Practice for the Care and Use of Animals for Scientific Purposes.

Cell lines

Ovarian cancer cell lines were obtained from the National Cancer Institute Repository, actively passaged for less than 6 months, and authenticated using short-tandem repeat markers

to confirm their identity against the Cancer Genome Project database (Wellcome Trust Sanger Institute, Cambridgeshire, United Kingdom) before use in experiments. Cells were maintained at 37°C and 5% CO₂ (v/v), and cultured in RPMI1640 media containing 10% (v/v) FCS and 1% penicillin/streptomycin. Transfection and drug sensitivity assays were performed in the absence of antibiotics. Cell lines resistant to dinaciclib were generated utilizing methods as described previously (13). Briefly, OVCAR3 cells were plated in 6-well plates and treated with dinaciclib at the IC₅₀ dose for two 72-hour periods (media removed and fresh drug added). Surviving cells were allowed to repopulate for 96 hours and the process repeated once. Remaining cells were cultured in media or in the presence of drug, and regularly monitored for sensitivity to dinaciclib. Six independent cell lines were generated in this fashion, and designated OVCAR3-RD1 to -RD6.

Short hairpin-mediated *CDK2* knockdown

Short hairpin-mediated knockdown of *CDK2* was performed by cloning *CDK2*-specific shRNA into a lentiviral tetracycline-inducible expression vector containing the optimized miR-E backbone (18). The modified lentiviral vector pRRL-T3G-TurboGFP-miRE-PGK-mCherry-IRES-rTA3 (also referred to as LT3GECIR) system includes a red (mCherry) fluorescent marker for transduction and a green (turboGFP) fluorescent marker for induction. Five *CDK2*-specific shRNA constructs were cloned into this system (see Supplementary Table S2 for sequences). For lentiviral production, HEK293T cells were transfected with plasmid DNA combined with the Lenti-X packaging system (Clontech Laboratories). Transfection, production of lentiviral particles, and transduction of target cells was performed as described by the manufacturer's protocol. Doxycycline was used to induce shRNA expression, and transfection efficiency was validated by flow cytometry (FACS), and knockdown of individual hairpins by RT-PCR and Western blot analysis. The most efficient shRNA construct was taken forward for *in vitro* and *in vivo* experiments.

For *in vivo* experiments, xenograft tumors from transduced cells were generated as described below. Once tumors reached 100 mm³, mice were randomized into two groups to receive either normal food and water or doxycycline food and water (2 mg/mL in 2% sucrose) as a means of reliable induction of shRNA expression. Tumors were subsequently monitored as described below.

Cyclin E1 and AKT overexpression in Fallopian tube secretory epithelial cells

The immortalized fallopian tube secretory epithelial cell (FTSEC) line FT282 was obtained from Ronny Drapkin (University of Pennsylvania, Philadelphia, PA; ref. 19). Derivative cell lines were generated using pMSCV-mCherry-(empty) and pMSCV-mCherry-*CCNE1*, encoding full-length *CCNE1*. Additional cell lines were generated with pMSCV-GFP-myr-AKT1, pMSCV-GFP-myr-AKT2, and pMSCV-GFP-myr-AKT3, encoding the three different isoforms of myr-AKT (20). Plasmids were validated by sequencing, and expression of *CCNE1*, *AKT1*, *AKT2*, and *AKT3* was validated by quantitative real-time PCR and Western blotting. Primer sequences are listed in Supplementary Table S1.

High-throughput compound screen

The compound library consisted of 73 targeted agents, 71 epigenetic agents, 208 kinase inhibitors, and 3,707 known drugs

(21). All agents were dissolved in DMSO, and diluted to concentrations from 0.01 to 10 $\mu\text{mol/L}$. For targeted agents, epigenetic agents and kinase inhibitors, the primary screen was conducted using 11 concentrations; for the known drug library three concentrations were used. Compounds were dispensed into 384-well drug stock plates and stored at -20°C . Stock plates for dinaciclib at a fixed dose concentration (EC_{30}) were prepared using a multichannel pipette before each assay.

Early passage cells were deposited into 384-well microtiter plates at 750–1,500 cells per well using a multidrop dispenser (Thermo Scientific) in 40 μL of media. Cells were allowed to adhere overnight. A MiniTrak IX (PerkinElmer Life Sciences) automated robotic platform was used to dispense compounds into assay plates. Compounds were added directly to assay plates using a 384, hydrophobic slotted pintool (VP Scientific) calibrated to dispense 0.1 μL of DMSO compound solution. DMSO (0.1%) was used as negative control. Cells were exposed to drug for 48 hours, and cell viability measured using the CellTiter-Glo Luminescent Assay (Promega) using the EnVision Multilabel Plate Reader (PerkinElmer). Average viability was normalized to DMSO control wells, and EC_{50} dose was approximated by fitting a four-parameter dose–response curve using XLfit (IDBS).

Xenograft studies

Estrogen pellets were implanted subcutaneously into 4- to 6-week-old female NOD/SCID mice to facilitate the growth of xenografted cells. The pellet was implanted 3 days before injection of cells. Cell lines were grown *in vitro*, washed twice with PBS, and resuspended in 50% Matrigel (BD Biosciences) in PBS. Mice were injected subcutaneously with 5×10^6 cells in 100 μL , and monitored at least twice weekly. Tumor volume was calculated using the equation: $\text{volume} = (\text{width})^2 \times \text{length}/2$. When tumors reached 100 to 150 mm^3 , mice were randomized into groups of five for treatment with vehicle alone or drug. Dinaciclib was prepared fresh before injection in 20% (w/v) hydroxypropyl-beta-cyclodextrin (Cyclodextrin Technologies Development, Inc.) and mice dosed twice weekly as a single agent via intraperitoneal injection. MK-2206 was reconstituted in 30% (w/v) Captisol (Ligand Technology) and dosed at 60 mg/kg three times per week as a single agent via oral gavage. For combination studies, MTDs of dinaciclib 20 mg/kg and MK-2206 60 mg/kg were dosed three times per week. All mice were monitored daily following drug dosing. Tumors were harvested at specific time points for biomarker analysis or at study endpoint, with half snap frozen in liquid nitrogen and half fixed in formalin and paraffin embedded for IHC. Percentage tumor growth inhibition (TGI) was calculated as $100 \times (1 - \Delta\text{T}/\Delta\text{C})$ where ΔC and ΔT were determined by subtracting the mean tumor volume (in the vehicle control and treated groups, respectively) on day 1 of treatment, from the mean tumor volume on each day of assessment. Statistical analyses were performed using GraphPad Prism Version 6.0 (GraphPad) with ANOVA followed by Dunnett *post hoc* test to compare the tumor growth between treatment groups.

CCNE1 and AKT status in primary ovarian tumor samples

Genomic alterations identified in *CCNE1* and genes involved in the PI3K–AKT–mTOR pathway were obtained from The Cancer Genome Atlas (TCGA) cBioPortal (22, 23). All available data as of March 2015 were analyzed, comprising 316 primary ovarian serous cystadenocarcinoma samples (7).

shRNA screen data

Data from the Project Achilles was obtained to evaluate the interaction between *CCNE1*-amplified ovarian cancer cell lines and genes in the AKT pathway (24). Cell line copy number data were obtained from the Cancer Cell Line Encyclopedia (25). Only cell lines known to resemble HGSC according to their genomic characteristics (26) were used in the analysis ($N = 14$, see Supplementary Table S3). Cell lines with a \log_2 copy number ratio > 0.3 over the *CCNE1* locus were designated as amplified ($n = 9$) and cell lines with a \log_2 copy number ratio < 0 were designated as unamplified ($n = 5$). Cell lines with *CCNE1* gene expression greater than the median +1 SD ($n = 9$) were defined as *CCNE1*-high expression, whereas cell lines with *CCNE1* gene expression less than median ($n = 5$) were defined as *CCNE1*-low expression.

Additional methods for gene suppression studies, Western blot analysis, IHC, flow cytometry and drug sensitivity, clonogenic, proliferation, and anchorage-independent growth assays can be found in Supplementary Methods.

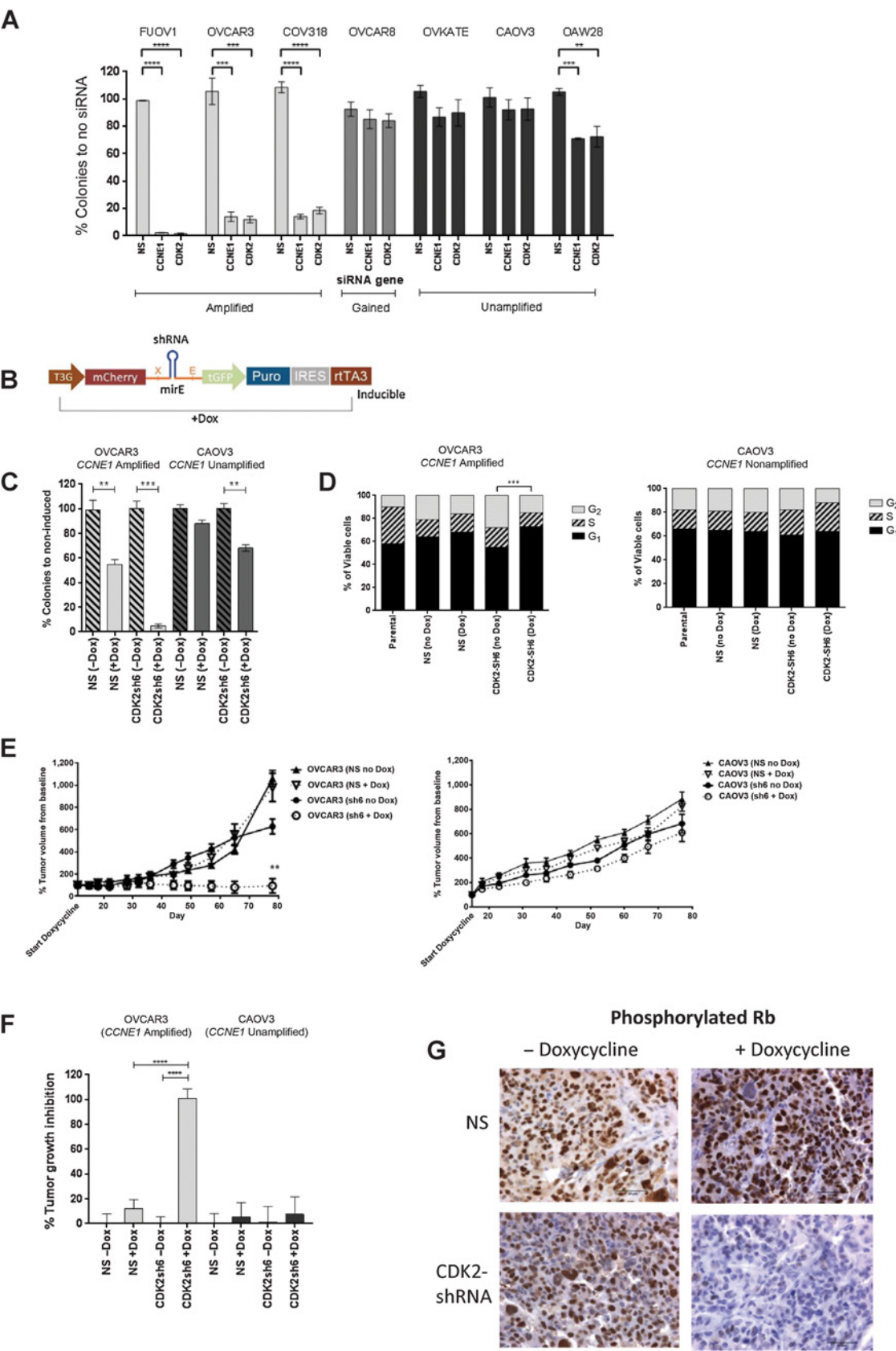
Results

CCNE1-amplified HGSC cells are selectively sensitive to CDK2 knockdown

We previously demonstrated in a limited number of cell lines that *CCNE1*-amplified HGSC cell lines are selectively sensitive to *CCNE1* and *CDK2* knockdown mediated by siRNA (13). Following a recent analysis of ovarian cancer cell lines (26), we extended our analysis to a wider number of HGSC cell lines and confirmed consistent amplicon-dependent sensitivity to siRNA-mediated *CCNE1* and *CDK2* knockdown (Fig. 1A and Supplementary Fig. S1A and S1B). The OVCAR8 cell line has a low-level gain of *CCNE1* and was not sensitive to *CCNE1* or *CDK2* knockdown (Fig. 1A). However, OVCAR8 does not overexpress cyclin E1 at the mRNA or protein level (Supplementary Fig. S1B and S1C) compared with other cell lines such as OVCAR4 that have similar *CCNE1* copy number. These findings suggest a threshold of *CCNE1*/*CDK2* dependency that may be relevant to patient selection in clinical trials targeting this oncogene in HGSC.

To validate the effect of *CDK2* knockdown, we utilized a tetracycline-inducible shRNA targeting *CDK2* (Fig. 1B). Consistent with the siRNA data, inhibition of *CDK2* by shRNA resulted in reduced clonogenic survival, more evident in the *CCNE1*-amplified cell line, OVCAR3 compared with the *CCNE1*-unamplified cell line CAOV3 (Fig. 1C). Knockdown of *CDK2* was validated at the protein level (Supplementary Fig. S2A). Cell-cycle analysis demonstrated arrest in G_1 , seen only in the OVCAR3 cell line (Fig. 1D). We did not observe significant levels of apoptosis following *CDK2* knockdown, as assessed by percentage of Annexin V-positive cells measured by FACS (Supplementary Fig. S2B).

Cells transduced with *CDK2*-shRNA were grown as xenografts in NOD/SCID mice to examine the effects of *CDK2* knockdown *in vivo*. Consistent with the *in vitro* data, attenuation of *CDK2* expression in the OVCAR3 xenograft model resulted in significant tumor growth arrest in the group receiving doxycycline in food and water compared with controls (Fig. 1E–F). Induction of shRNA by doxycycline was monitored by *CDK2* gene expression measured by RT-PCR (Supplementary Fig. S2C). Reduced Rb1 phosphorylation was observed following *CDK2* knockdown in OVCAR3 tumors harvested at 7 days following induction (Fig. 1G), providing a biomarker of targeting cyclinE1/*CDK2*.



Taken together, *CCNE1*-amplified HGSC appear selectively sensitive to siRNA- and shRNA-mediated knockdown of *CDK2* both *in vitro* and *in vivo*. These findings support our previous studies and point to *CDK2* as a potential therapeutic target in *CCNE1*-amplified HGSC.

CDK2 inhibitor dinaciclib delayed tumor growth in *CCNE1*-amplified HGSC xenografts

Consistent with siRNA data, we previously showed in a limited number of cell lines selective sensitivity of *CCNE1*-amplified cell lines to dinaciclib, a potent *CDK2* inhibitor in advanced clinical development (13). However, in this study, when tested across a broader panel of HGSC cell lines, there did not appear to be a clear amplicon-dependent sensitivity (Fig. 2A), in contrast with the siRNA and shRNA data. Furthermore, activity *in vivo* was also seen in a xenograft model developed from a *CCNE1*-unamplified cell line, CAOV3 (Fig. 2A–D). The difference in amplicon-dependent sensitivity between gene suppression and pharmacologic inhibition may be due to the broad activity of dinaciclib, which, in addition to inhibiting *CDK2*, is also active against *CDK1*, 5, 9, and 12 (17, 27).

In addition to *CDK2* inhibitors, we previously identified use of bortezomib, a proteasome inhibitor, as a potential therapeutic strategy for *CCNE1*-amplified HGSC (12). Although we did not observe amplicon-dependent sensitivity to dinaciclib, we investigated the interaction between dinaciclib and bortezomib to see whether the two drugs would be synergistic in combination. Using the Chou–Talalay methodology for drug combination studies (28), we did not observe a synergistic interaction with dinaciclib and bortezomib (Fig. 2E and F) in a panel of *CCNE1*-amplified and *CCNE1*-unamplified HGSC cell lines. Given this lack of synergism, we sought to identify selective synergistic drug combinations by adopting an unbiased high-throughput screening approach.

A high-throughput compound screen identifies synergistic drug combinations

We performed a high-throughput compound screen to identify combinations that would be synergistic in *CCNE1*-amplified cells, as well as combinations that would be selective in a *CDK* inhibitor-resistant cell line OVCAR3-R1-533533 (13). In the primary screen, 4,059 compounds (including duplicates) were combined with a fixed dose of dinaciclib as described in Materials and Methods. Dose–response curves were generated and manually

curated, and compounds where a curve could not be fitted were excluded from the analysis. A full list of EC_{50} values for each cell line and compound is given in Supplementary Tables S4 and S5.

EC_{50} values from the primary screen were used to make two pair-wise comparisons (Fig. 2G and H): (i) dinaciclib plus library compound comparing OVCAR3 (*CCNE1*-amplified) versus SKOV3 (*CCNE1*-unamplified) and (ii) dinaciclib plus library compound comparing OVCAR3 (parental) and OVCAR3-R1 (*CDK* inhibitor resistant). At the time of undertaking the screen, SKOV3 was a commonly used ovarian cancer cell line; however, recent studies have demonstrated that SKOV3 is unlikely to resemble HGSC (26). Therefore, any potential hits identified in the screen were subsequently validated using only HGSC cell lines.

Library compounds where the ratio of EC_{50} was less than 0.5 were selected as hits for a secondary screen involving a total of 64 compounds (Supplementary Table S6 and S7). Compounds that appeared to have an additive effect with dinaciclib were selected as hits from the secondary screen and carried forward for further testing.

The final part of the screen involved assessing the level of synergy between the library compound hits and dinaciclib involving an 11-point titration of each compound. Using the Chou–Talalay methodology of constant-ratio drug combinations, a series of combination indexes were generated to identify synergistic interactions.

In the OVCAR3 parental cell line, there were no synergistic combinations identified between dinaciclib and the library compounds (Supplementary Table S8). In the OVCAR3-R1 cell line, there were a number of synergistic interactions identified (Supplementary Table S8). Nonselective BH3-mimetic agents ABT-263 and ABT-737 were synergistic in combination with dinaciclib, suggestive of a class effect. This was validated further in an independently derived dinaciclib-resistant cell line, OVCAR3-RD6 (Fig. 3A–B and Supplementary Fig. S4A–S4C). There was no synergistic interaction noted in the combination between dinaciclib and ABT-199 (Fig. 3C), a selective Bcl-2 antagonist. The combination of dinaciclib and ABT-737 resulted in a dose-dependent increase in apoptosis, observed only in *CDK* inhibitor-resistant cell lines as demonstrated by increase in PARP cleavage products on Western blot analysis (Fig. 3D). Mcl-1 protein expression was not observed in the OVCAR3-RD6 cell line resistant to dinaciclib (Fig. 3D). Real-time PCR demonstrated upregulation of antiapoptotic genes in the dinaciclib and

Figure 1.

CDK2 knockdown via siRNA and shRNA *in vitro* and *in vivo* results in selective reduction in clonogenic survival and tumor growth arrest in *CCNE1*-amplified HGSC. A, Clonogenic survival after transfection with *CCNE1* and *CDK2* siRNAs in panel of HGSC cell lines. Average percentage of discrete colonies formed after 7 to 10 days relative to no siRNA controls shown ($n = 3$). Error bars, SEM. Statistical significance (t test) calculated by comparison with nonsilencing (NS) siRNA in the same cell line. **, $P < 0.01$, ***, $P < 0.001$, ****, $P < 0.0001$. B, Schematic of conditional LT3GECIR lentiviral vector showing inducible transcripts produced by vector. C, Clonogenic survival after induction of a nonspecific or *CDK2*-targeting shRNA in OVCAR3 (*CCNE1*-amplified) and CAOV3 (*CCNE1*-unamplified). The average percentage of discrete colonies formed after 7 to 10 days relative to no induction shown ($n = 3$). Statistical significance (t test) calculated by comparison with noninduced (–Dox) in the same cell line; **, $P < 0.01$, ***, $P < 0.001$. D, Cell-cycle analysis following *CDK2* knockdown with inducible shRNA. Proportion of cells in G_1 , S , or G_2 phase for propidium iodide (PI)-stained cells analyzed by flow cytometry 72 hours after induction with doxycycline. Mean of three independently performed experiments shown. Statistical significance (t test) calculated by comparison with noninduced (–Dox) in the same cell line. ***, $P < 0.001$. E, Mean percentage change in tumor volume \pm SEM following induction of a nonspecific (NS) or *CDK2* (sh6) shRNA in subcutaneous xenograft tumors grown in immunocompromised mice, generated from OVCAR3 and CAOV3. Induced and noninduced groups as marked, $n = 5$ per group. **, $P < 0.001$, unpaired t test comparison of mean percentage tumor volume change. F, Percentage tumor growth inhibition following induction of nonspecific (NS) or *CDK2* (sh6) shRNA with doxycycline. Bars, mean \pm SEM, $n = 5$ mice per group. Statistical analysis performed with ANOVA followed by Dunnett *post hoc* test to compare the percentage tumor growth inhibition between the treatment groups. ****, $P < 0.0001$. G, IHC assessment of phospho-Rb with or without doxycycline treatment in OVCAR3 xenograft tumor.

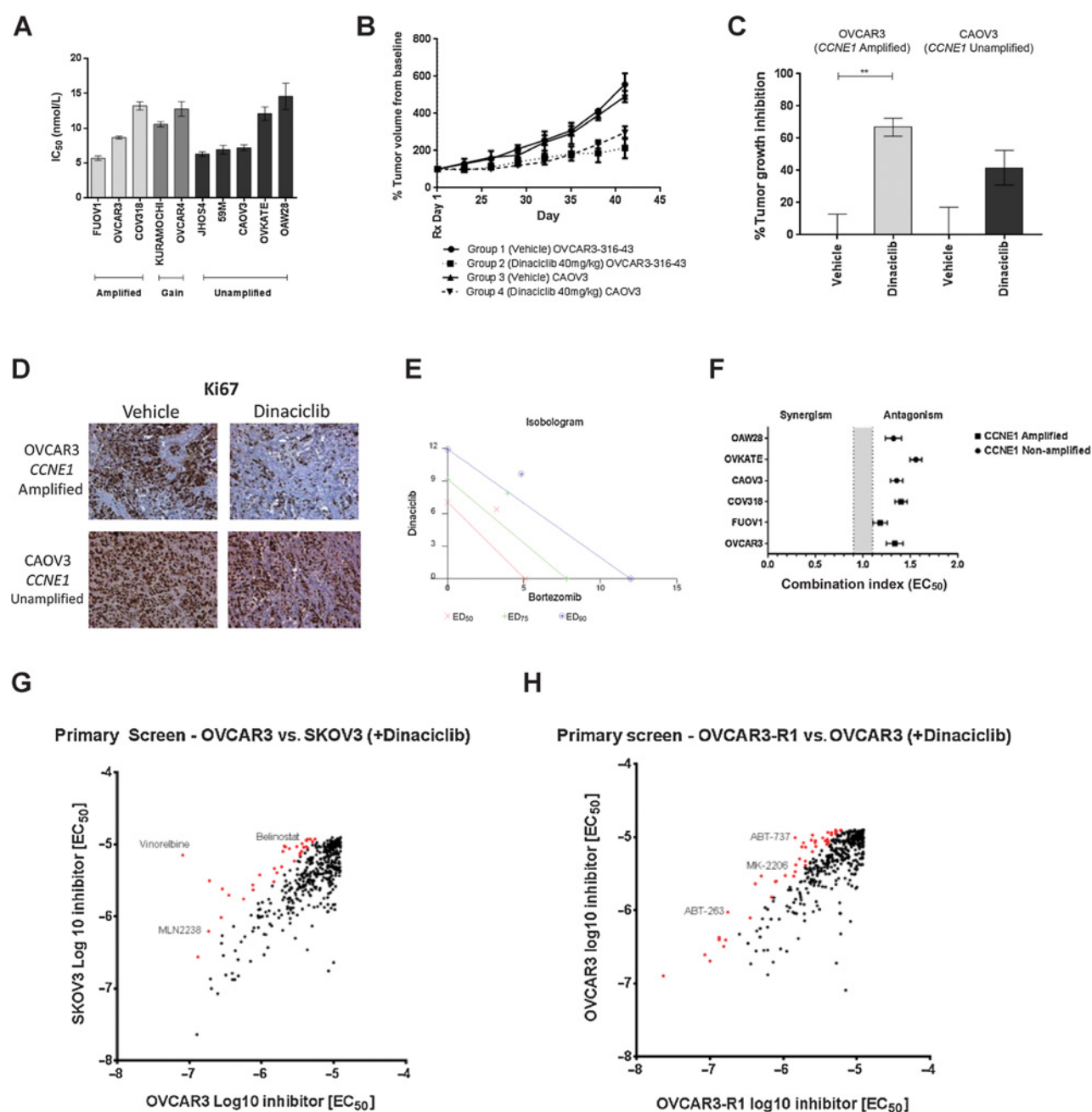
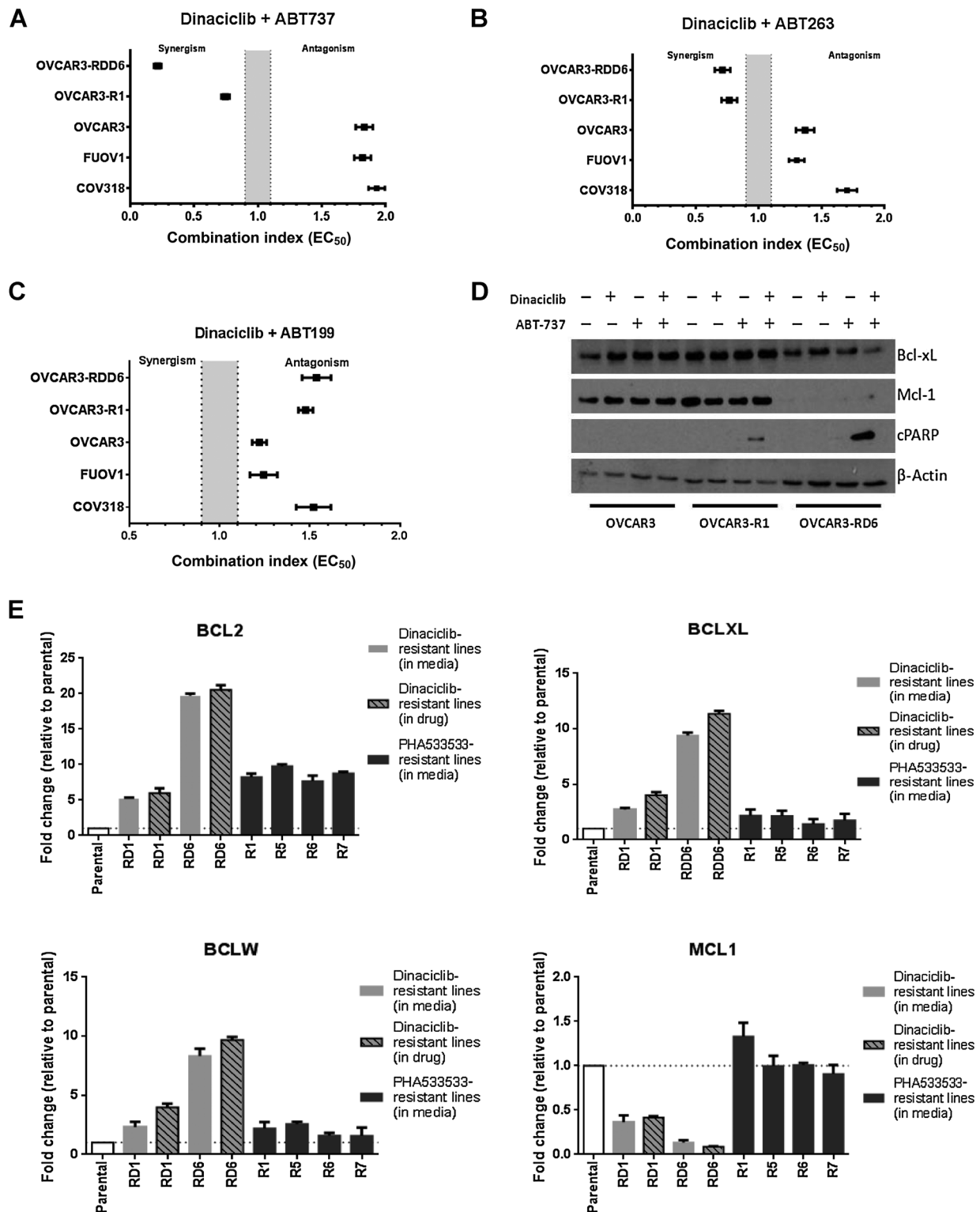


Figure 2.

CDK inhibitor dinaciclib results in modest tumor growth inhibition *in vivo* but is not synergistic in combination with bortezomib *in vitro*. **A**, Mean IC₅₀ values for a panel of HGSC cell lines treated with dinaciclib generated from dose-response curves following standard MTS cell proliferation assays. Error bars, SEM, $n = 3$ experiments. **B**, *In vivo* effects of dinaciclib. Immunocompromised mice bearing OVCAR3 (CCNE1-amplified) or CAOV3 (CCNE1-unamplified) tumor xenografts were treated with vehicle or drug as described in Materials and Methods. Plots represent mean tumor volume change from baseline \pm SEM, $n = 5$ mice per group. **C**, the percentage tumor growth inhibition following 21 days of treatment with vehicle or dinaciclib. Bars represent mean \pm SEM, $n = 5$ mice per group. Statistical analysis performed with ANOVA followed by Dunnett *post hoc* test to compare the percentage tumor growth inhibition between the treatment groups. **, $P < 0.01$. **D**, Immunohistochemical analysis of Ki67 expression in OVCAR3 and CAOV3 tumor xenograft harvested 24 hours after dose of vehicle or dinaciclib. **E**, Formal assessment of synergy between dinaciclib and bortezomib using Chou-Talalay Isobologram analysis. Figures are generated with CalcuSyn 2.0. Data are normalized, with connecting line at X and Y corresponding to combination index = 1, representing line of additivity. Data points above the line are antagonistic, along or near the line are additive and points below the line are synergistic. **F**, Combination indexes for a panel of HGSC cell lines tested against dinaciclib in combination with bortezomib. Values represent mean \pm SEM, $n = 3$. **G-H**, Scatter plots showing EC₅₀ values for library compounds in combination with dinaciclib from primary screen for the comparison between CCNE1-amplified and unamplified (G) and resistant versus parental (H). Data points in red represent compounds taken forward for secondary screen.

**Figure 3.**

Dinaciclib in combination with nonselective BH3 mimetics are synergistic in CDK inhibitor-resistant cell lines. Combination indexes for parental and CDK inhibitor-resistant cell lines tested against dinaciclib in combination with ABT-737 (A), ABT-263 (B), ABT-199 (C). Values represent mean \pm SEM, $n = 3$. D, Western blot analysis demonstrating protein expression of Bcl-XL, Mcl-1, and PARP cleavage products in OVCAR3 parental and CDK inhibitor-resistant cell lines after treatment with dinaciclib and ABT-737. E, Expression of antiapoptotic proteins as assessed by quantitative real-time PCR. R-lines signify cell lines resistant to PHA533533. RD lines signify cell lines resistant to dinaciclib. Bars represent mean \pm SEM, $n = 3$.

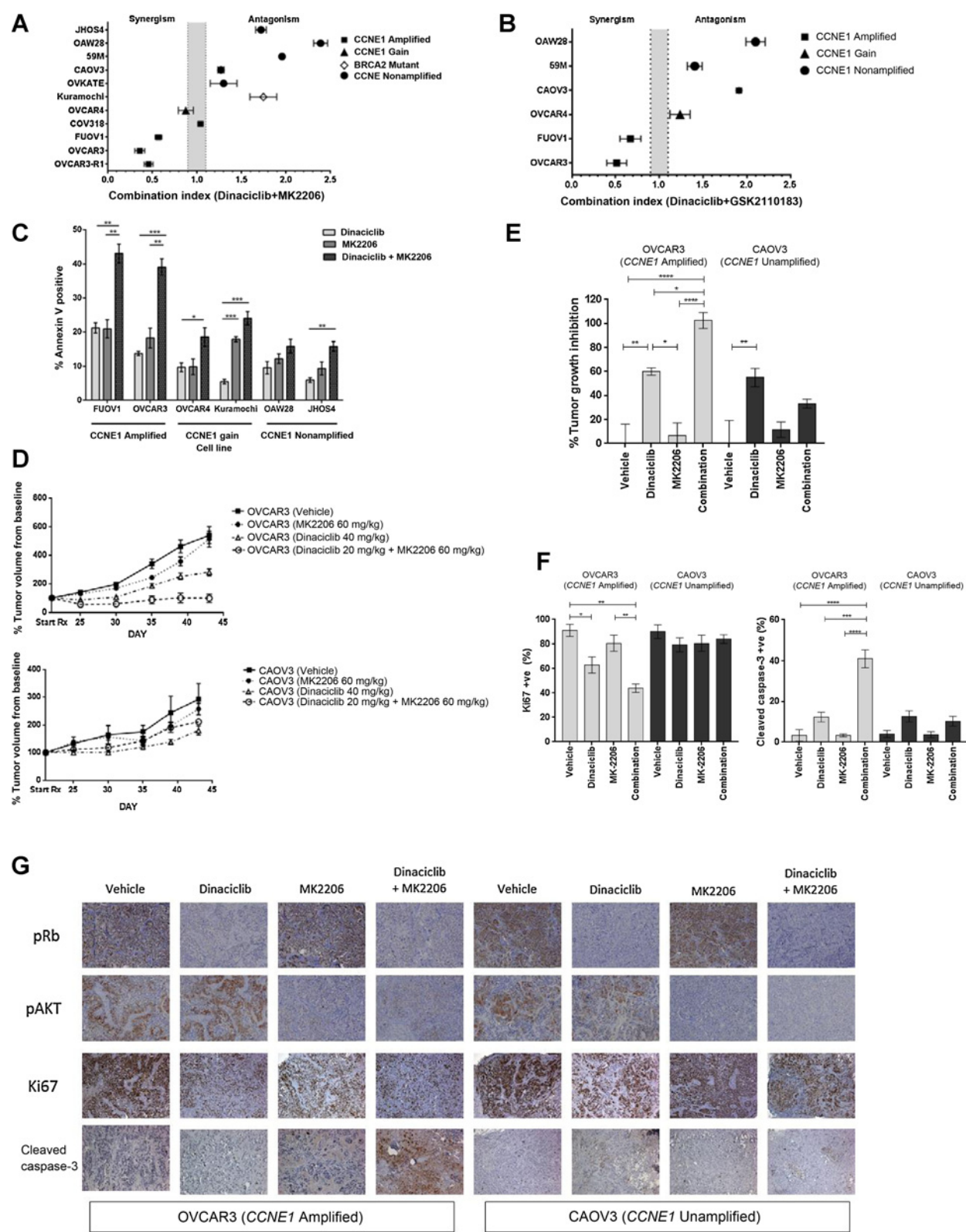


Figure 4. Dinaciclib in combination with two AKT inhibitors are synergistic *in vitro* and *in vivo* models of *CCNE1*-amplified HGSC. Combination indexes for a panel of HGSC cell lines tested against dinaciclib in combination with MK-2206 (A) and GSK2110183 (B). Values represent mean \pm SEM, (Continued on the following page.)

PHA533533-resistant cell lines (Fig. 3E), but downregulation of *MCL1* in the dinaciclib-resistant OVCAR3-RD cell lines. Dinaciclib is reported to have a greater effect on CDK9 compared with PHA533533 (13). Given that *MCL1* is regulated by CDK9 activity (29), this may explain the reduction of *MCL1* levels in the presence of dinaciclib. However, it is unclear why reduced *MCL1* expression is also apparent in OVCAR3-RD cell lines even when grown in the absence of dinaciclib.

MK-2206, a pan-AKT inhibitor, was identified as a synergistic drug combination in the CDK inhibitor-resistant cell line, OVCAR3-R1. In validating this interaction between dinaciclib and MK-2206, we observed that this combination was also synergistic in *CCNE1*-amplified cell lines FUOV1 and parental OVCAR3 (Fig. 4A). This effect was similarly observed with another AKT inhibitor, GSK-2110183 (Fig. 4B), that was not included in the original high-throughput screen library. Exposure to dinaciclib and MK2206 resulted in significantly higher number of apoptotic cells in *CCNE1*-amplified cell lines, indicated by percentage of Annexin V-positive cells measured by FACS (Fig. 4C). This result was similarly observed on Western blot analysis, with appearance of PARP cleavage products following treatment of OVCAR3 cells with the combination of dinaciclib and MK-2206 (Supplementary Fig. S4D). As dinaciclib targets several CDKs in addition to CDK2 (17), we used siRNA knockdown of CDK2, CDK1, or CDK9 to determine the specificity of the synergistic effect of dinaciclib and MK-2206. We found that the synergy observed was predominantly mediated through CDK2 (Supplementary Fig. S4E).

Dinaciclib and MK-2206 are selectively synergistic in *CCNE1*-amplified cell lines *in vivo*

The *in vivo* effect of dinaciclib and MK-2206 was assessed using xenograft models from *CCNE1*-amplified and unamplified cell lines, OVCAR3 and CAOV3, respectively. The combination was significantly more effective than each single agent alone in the *CCNE1*-amplified model (Fig. 4D and E), whereas there was no statistically significant effect of the combination compared to single-agent treatment in the *CCNE1*-unamplified model. After a treatment period of three weeks with dinaciclib and MK-2206, xenograft tumors began regrowing within 10 days of treatment cessation. Rechallenge with the same drug combination resulted in significant tumor regression (Supplementary Fig. S4F), indicating continued sensitivity to the combination. Consistent with this effect on tumor growth, treatment with dinaciclib and MK-2206 resulted in inhibition of cell proliferation and induction of apoptosis, as assessed by Ki67 and cleaved caspase-3 IHC on tumors harvested at 24 hours (Fig. 4F and G). Taken together, the high-throughput screen identified a novel combination of dina-

ciclib and MK-2206 that appeared to be selectively synergistic in *CCNE1*-amplified HGSC cell lines both *in vitro* and *in vivo*.

CCNE1 and *AKT2* are frequently coamplified in primary HGSC samples

We sought to investigate whether there was evidence for an interaction between *CCNE1* amplification and the AKT pathway in primary tumor samples. Analysis of TCGA dataset indicated that *CCNE1* and *AKT2* amplification events cooccur ($P < 0.001$; Supplementary Fig. S5). This observation was not seen with other isoforms of AKT or genes in the AKT pathway. To examine the relationship between *CCNE1* amplification and the AKT pathway further, we made use of data from Project Achilles, a genome-wide shRNA screen of synthetic lethality in 216 cancer cell lines (24). The abundance of shRNA sequence relative to a reference pool was measured by microarray to identify genes essential for survival. We analyzed the effect of shRNA-targeting genes within the AKT pathway, restricting the analysis to HGSC cell lines, classified according to *CCNE1* copy number or expression. A statistically significant dependence on genes in the AKT pathway, including *AKT2*, was observed, indicated by a depletion of shRNAs targeting these genes in cell lines with *CCNE1* amplification or overexpression (Fig. 5). *CDK2* was included in the analysis as a control, and consistent with our previous analysis, was shown to be required in *CCNE1*-amplified cells (13).

Cyclin E1 and AKT overexpression cooperates to promote uncontrolled growth in FTSECs

Previously, Karst and colleagues demonstrated that cyclin E1 overexpression combined with *TP53* mutation in FTSECs resulted in increased proliferation, colony-forming ability, and colony formation in soft agar (19). However, cyclin E1 overexpression alone did not result in complete transformation, suggesting that additional events are required.

We examined the interaction between cyclin E1 and AKT overexpression in FTSECs by overexpressing the myristoylated, active forms of AKT1, AKT2, and AKT3 (20). Expression of each AKT isoform and cyclin E1 was validated with Western blot analysis (Fig. 6A) and RT-PCR (Supplementary Fig. S6A). Overexpression of AKT isoforms led to increased expression of AKT downstream targets (Supplementary Fig. S6B). AKT2 and cyclin E1 overexpression alone or in combination showed a trend toward increased proliferation compared with empty vector alone (Fig. 6B), and AKT2 or AKT3 overexpression in combination with cyclin E1 showed a trend toward enhanced clonogenic colony formation in comparison with overexpression of cyclin E1 alone (Fig. 6C). There was a significant increase in soft agar colony formation with the overexpression of AKT2 or AKT3 in combination with

(Continued.) $n = 3$. C, HGSC cell lines were cultured *in vitro* with dinaciclib, MK-2206, or the combination for 24 hours and then analyzed using flow cytometry for Annexin V/propidium iodide positivity. Bars, mean \pm SEM, $n = 3$. *, $P < 0.05$; **, $P < 0.01$; ***, $P < 0.001$; unpaired *t* test. D, *In vivo* effects of vehicle, dinaciclib, MK-2206, or combination. Immunocompromised mice bearing OVCAR3 (*CCNE1*-amplified) or CAOV3 (*CCNE1*-unamplified) tumor xenografts were treated with vehicle or drug as described in Materials and Methods. Plots represent mean tumor volume change from baseline \pm SEM, $n = 5$ mice per group. E, Percentage tumor growth inhibition following 21 days of treatment with vehicle, dinaciclib, MK-2206, or the combination. Bars, mean \pm SEM, $n = 5$ mice per group. Statistical analysis performed with ANOVA followed by Dunnett *post hoc* test to compare the percentage tumor growth inhibition between the treatment groups. *, $P < 0.05$; **, $P < 0.01$; ***, $P < 0.0001$. F, Quantitation of immunohistochemical staining for Ki67 and cleaved caspase-3. Bars, mean percentage of Ki67 or cleaved caspase-3-positive cells relative to background number of cells measured \pm SEM, $n = 3$ in each group. Statistical analysis performed by ANOVA with Tukey multiple comparison test to compare between treatment groups. G, Subcutaneous tumors were obtained after 24 hours of treatment and were examined by IHC for biomarker analysis. Rb phosphorylation was inhibited by dinaciclib, but not MK-2206 treatment. AKT phosphorylation was inhibited by MK-2206, but not dinaciclib treatment. Proliferation (Ki67) was inhibited and apoptosis (cleaved caspase-3) was induced by the combination of dinaciclib and MK-2206 in *CCNE1*-amplified xenograft model (OVCAR3).

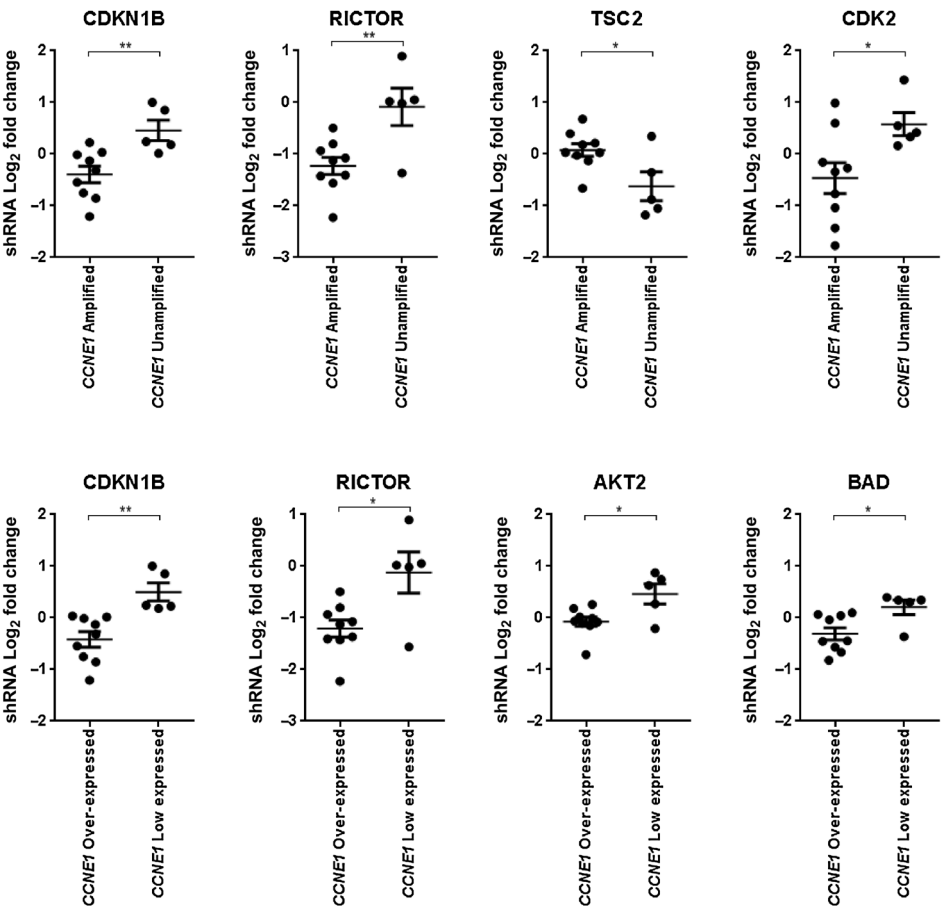


Figure 5. CCNE1 and AKT2 are coamplified in primary HGSC samples. Dot plots of median shRNA abundance for each gene targeted by shRNA in HGSC cell lines, stratified by CCNE1 copy number or expression. Depletion of shRNA abundance within a group suggests requirement for maintained expression of its target gene. Only genes with a statistically significant difference are shown; see Supplementary Table S3 for the list of genes and cell lines analyzed. Statistical significance (*t* test) calculated by comparison between CCNE1-amplified and unamplified or CCNE1 overexpressing and low expressing cell lines; *, *P* < 0.05; **, *P* < 0.01.

cyclin E1 compared with overexpression of cyclin E1 alone (Fig. 6D). These findings support an interaction between cyclin E1 and AKT pathway to promote uncontrolled growth in FTSECs, and may explain synergism observed between dinaciclib and MK-2206 in CCNE1-amplified HGSC.

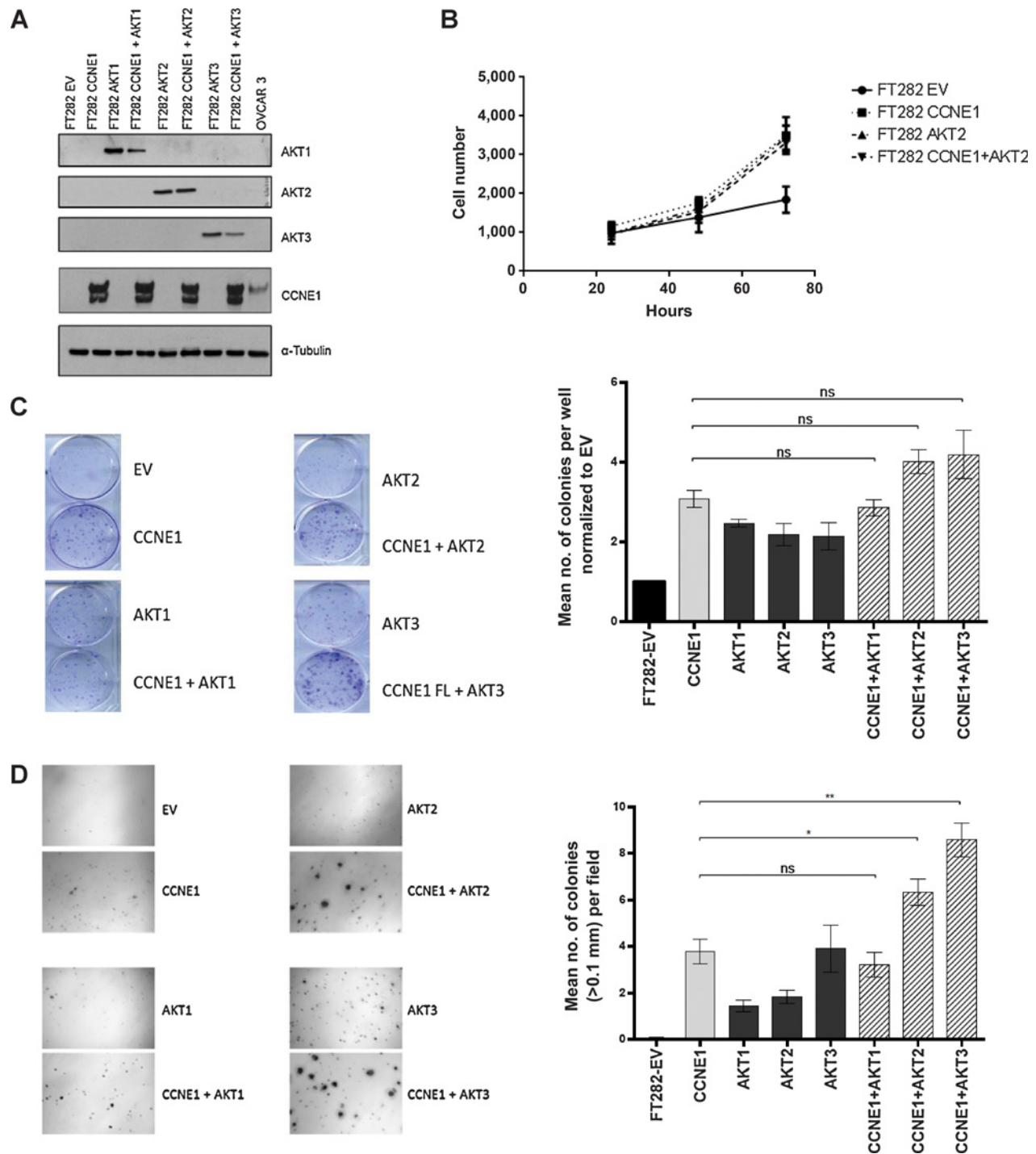
Discussion

HGSC patients with CCNE1 amplification have a clear unmet need in terms of effective therapies. In this study, we validate CDK2 as a selective target in CCNE1-amplified HGSC using shRNA-mediated gene suppression *in vitro* and *in vivo*. However, we did not observe similar amplicon-dependent specificity to dinaciclib, a small-molecule inhibitor targeting CDKs. This may be due to the nonspecificity of inhibitors such as dinaciclib or a role for kinase-independent activities of CCNE1 in amplified HGSC (30). Our findings highlight the potential differences between inhibition of kinase activity and complete suppression of CCNE1 or CDK2 gene expression.

In addition to CDK2, dinaciclib targets CDK1, 5, 9, and 12 (17, 27). CDK9 phosphorylates the carboxyl-terminal repeat domains of RNA polymerase II, and inhibition of CDK9 by dinaciclib results in rapid downregulation of mRNA transcripts and proteins with short half-lives such as the antiapoptotic BCL2 family member, Mcl1 (17). Preclinical studies have indicated dinaciclib-mediated targeting of Mcl-1 may be an effective therapeutic approach in a number of different cancers (17). Inhibition

of CDK2 kinase activity may also differ significantly from complete suppression of gene expression, resulting in varying downstream and compensatory effects (31, 32). Studies with knockout experiments indicate that CDK2 functions appear redundant with CDK1, although in our studies, we did not observe upregulation of CDK1 expression following CDK2 knockdown *in vitro* or *in vivo* (data not shown).

Although we observed a difference in the amplicon-dependent sensitivity of CDK2 gene suppression compared with pharmacologic inhibition, dinaciclib remains a potent CDK2 inhibitor with single-agent activity in CCNE1-amplified HGSC cell lines and is one of the most clinically advanced CDK2 inhibitors (33). Therefore, to more effectively target CCNE1-amplified HGSCs, we performed a combinatorial drug screen to identify compounds that would synergize with dinaciclib. We also sought to identify compounds that may potentially overcome resistance to dinaciclib, a common occurrence in the clinical use of targeted small-molecule inhibitors, by testing a cell line that was resistant to CDK inhibitors. Dinaciclib in combination with MK-2206, an AKT inhibitor, was identified as a synergistic combination in targeting CDK inhibitor-resistant cell lines. This supported our previous work that identified increased AKT1 copy number and upregulation of genes in the AKT pathway as a potential mechanism of resistance to CDK2 inhibitors (13). In validating this finding, we observed selective, potent synergism between dinaciclib and MK-2206 *in vitro* and *in vivo* models of CCNE1-amplified HGSCs, including parental OVCAR3 cells. This interaction was not

**Figure 6.**

Cyclin E1 and AKT overexpression cooperates to promote uncontrolled growth in FTSECs. A, Western blot analysis of fallopian tube secretory cells transduced with cyclin E1, empty vector, and AKT1, AKT2, and AKT3 overexpression constructs. Blots are representative of three independently performed experiments. B, Proliferation assay of fallopian tube secretory cells (FT282) transduced with empty vector (EV), cyclin E1 (CCNE1), AKT2, and both cyclin E1 and AKT2 (CCNE1+AKT2). Plots represent mean of three independently performed experiments, error bars represent SEM. C, Clonogenic survival assay of FT282 cells transduced as labeled. Images (left) show cells fixed and stained with crystal violet. Bar chart represents mean of three independently performed experiments, error bars represent SEM. Statistical significance (*t* test) calculated by comparison with FT282 cells transduced with cyclin E1 (FT282-CCNE1). D, Anchorage-independent assay of FT282 cells transduced as labeled. Images (left) represent cells fixed with 2% paraformaldehyde and captured using an Olympus IX81 live cell imager. Bar chart represents mean of three independently performed experiments, error bars represent SEM. Statistical significance (*t* test) calculated by comparison with FT282 cells transduced with cyclin E1 (FT282-CCNE1); *, $P < 0.05$, **, $P < 0.01$.

initially observed in the primary high-throughput screen. However, the use of SKOV3 cell line as a comparator in the screen may be a potential confounder, as the selection of compounds as hits from the primary screen was based on a difference in the EC₅₀ values between the two cell lines tested, OVCAR3 and SKOV3. Recently, multiple studies characterizing the genomic profile of commercially available ovarian cancer cell lines have shown that many of these cell lines, including SKOV3, may not accurately resemble HGSC (26, 34–36).

Synergism between dinaciclib and MK-2206, as well as another AKT-specific inhibitor GSK2110183, but an absence of a synergistic combination with other inhibitors of the PI3K–AKT–mTOR pathway suggests that the interaction with *CCNE1* may be specific to AKT. Analysis of genomic data from patients demonstrated a significant cooccurrence of *CCNE1* and *AKT2* amplification, which may in part be explained by colocalization on chromosome 19q. However, FUV1, which has *CCNE1*-amplification without *AKT2*-amplification (25), was equally sensitive to the combination of dinaciclib and AKT inhibitors. Coexpression of *AKT2* or *AKT3* with cyclin E1 in a *TP53*-mutant FTSEC cell line resulted in increased proliferation and anchorage-independent growth. Analysis of data from Project Achilles indicates that HGSC cell lines that have *CCNE1* amplification or overexpression are dependent on multiple genes within the AKT pathway. We previously performed a pathway analysis of genes coexpressed with *CCNE1* amplification and observed an enrichment of genes involved in AKT signaling (12). Collectively, these data suggest a specific dependency of *CCNE1*-amplified tumors for AKT activity.

Dinaciclib and MK-2206 have previously been shown to be active against pancreatic adenocarcinoma (37). In *KRAS*-mutant pancreatic cancer patient–derived xenografts, Hu and colleagues (37) demonstrated efficacy of dinaciclib combined with MK-2206. They proposed that sensitivity was due to the effect of dinaciclib on CDK5, and in turn, inhibition of RAL pathway. On the basis of these results, a phase I clinical trial (NIH Trial NCT01783171) of dinaciclib and MK-2206 has been initiated in patients with advanced pancreatic cancer. While this trial will provide safety and recommended dosing of the combination, patients are not preselected on the basis of tumoral *CCNE1* amplification, and the mechanism of interaction and biomarkers that predict response are likely to be different in pancreatic cancer compared with HGSC.

Other combinations were also identified from the high-throughput screen. In particular, nonselective BH3-mimetic compounds ABT-737 and ABT-263 were synergistic in combination with dinaciclib in CDK inhibitor–resistant cell lines. There was no synergistic interaction between dinaciclib and the Bcl-2–specific antagonist, ABT-199, indicating that the targeting of multiple antiapoptotic proteins is potentially required to overcome resistance to CDK2 inhibitors. This observation is supported by upregulation of multiple genes in this pathway including BCL-2, BCL-XL, and BCL-W in resistant cell lines. However, the use of ABT-737 or ABT-263 in combination with dinaciclib *in vivo* is hindered by significant toxicities, particularly hematologic (Joel Levenson, personal communication), and are therefore unlikely to have clinical utility.

Biomarker-driven trials in HGSC are needed to improve clinical outcomes. HGSC patients with *CCNE1* amplification are a subset that requires different treatment approaches, given that they have HR-proficient tumors, and as such, are likely to have poor responses to platinum-based chemotherapy and PARP inhibitors. However, targeted therapies when used alone may not be sufficient

to induce selective, cytotoxic effects, and often result in the development of resistance. Combination therapies may potentially be a strategy to overcome these limitations. High-throughput drug screening is an unbiased approach to identify novel therapeutic strategies, and we have identified dinaciclib and MK-2206 as a combination that may prove to selectively target patients with *CCNE1*-amplified HGSC. Further work incorporating additional clinically relevant models and novel combinations will inform the design of rational clinical trials targeting *CCNE1*-amplified HGSC.

Disclosure of Potential Conflicts of Interest

No potential conflicts of interest were disclosed.

Authors' Contributions

Conception and design: G. Au-Yeung, W.J. Azar, C. Cullinane, D. Rischin, R. Drapkin, D. Etemadmoghadam, D.D.L. Bowtell

Development of methodology: G. Au-Yeung, F. Lang, W.J. Azar, K. Lackovic, R.B. Pearson, R. Drapkin

Acquisition of data (provided animals, acquired and managed patients, provided facilities, etc.): G. Au-Yeung, F. Lang, W.J. Azar, K.E. Jarman, K. Lackovic, D. Aziz

Analysis and interpretation of data (e.g., statistical analysis, biostatistics, computational analysis): G. Au-Yeung, F. Lang, W.J. Azar, K. Lackovic, C. Cullinane, D.D.L. Bowtell

Writing, review, and/or revision of the manuscript: G. Au-Yeung, F. Lang, C. Mitchell, K. Lackovic, C. Cullinane, R.B. Pearson, L. Mileskin, D. Rischin, D. Etemadmoghadam, D.D.L. Bowtell

Administrative, technical, or material support (i.e., reporting or organizing data, constructing databases): W.J. Azar, C. Mitchell, K.E. Jarman, R. Drapkin
Study supervision: L. Mileskin, D. Rischin, D. Etemadmoghadam, D.D.L. Bowtell

Other [created material integral to the study (engineered primary human cell lines)]: A.M. Karst

Acknowledgments

The authors wish to acknowledge staff from the Peter MacCallum Cancer Centre Animal facility, FACS facility, and Histology core facility for their assistance.

Grant Support

This work was supported by a National Health and Medical Research Council (NHMRC) program grant (APP1092856; to D.D.L. Bowtell), NHMRC project grant (APP1042358; to D. Etemadmoghadam), a Pfizer Cancer Research Grant (W180176; to G. Au-Yeung), University of Melbourne Australian Postgraduate Award (to G. Au-Yeung), the U.S. Army Medical Research and Materiel Command (OC140511; to D.D.L. Bowtell and R. Drapkin), the National Cancer Institute at the NIH (P50-CA083636 and R21 CA156021; to R. Drapkin); the Honorable Tina Brozman "Tina's Wish" Foundation (to R. Drapkin), the Dr. Miriam and Sheldon G. Adelson Medical Research Foundation (to R. Drapkin), a Canadian Institutes of Health Research Fellowship (to A.M. Karst), a Kaleidoscope of Hope Foundation Young Investigator Research grant (to A.M. Karst), the Basser Center for BRCA, and Department of Obstetrics and Gynecology at the University of Pennsylvania Perelman School of Medicine (to R. Drapkin). The Australian Ovarian Cancer Study is supported by the Peter MacCallum Cancer Centre Foundation, U.S. Army Medical Research and Materiel Command under DAMD17-01-1-0729, The Cancer Council Victoria, Queensland Cancer Fund, The Cancer Council New South Wales, The Cancer Council South Australia, The Cancer Foundation of Western Australia, The Cancer Council Tasmania, and the National Health and Medical Research Council of Australia (NHMRC; ID#628779), Stephanie Boldeman, the Agar family, and Ovarian Cancer Australia.

The costs of publication of this article were defrayed in part by the payment of page charges. This article must therefore be hereby marked *advertisement* in accordance with 18 U.S.C. Section 1734 solely to indicate this fact.

Received March 10, 2016; revised September 6, 2016; accepted September 12, 2016; published OnlineFirst xx xx, xxxx.

References

- Martini M, Vecchione L, Siena S, Tejpar S, Bardelli A. Targeted therapies: how personal should we go? *Nat Rev Clin Oncol* 2012;9:87–97.
- Burger RA, Brady MF, Bookman MA, Fleming GF, Monk BJ, Huang H, et al. Incorporation of bevacizumab in the primary treatment of ovarian cancer. *N Engl J Med* 2011;365:2473–83.
- Perren TJ, Swart AM, Pfisterer J, Ledermann JA, Pujade-Lauraine E, Kristensen G, et al. A phase 3 trial of bevacizumab in ovarian cancer. *N Engl J Med* 2011;365:2484–96.
- Fong PC, Boss DS, Yap TA, Tutt A, Wu P, Mergui-Roelvink M, et al. Inhibition of poly(ADP-ribose) polymerase in tumors from BRCA mutation carriers. *N Engl J Med* 2009;361:123–34.
- Ledermann J, Harter P, Gourley C, Friedlander M, Vergote I, Rustin G, et al. Olaparib maintenance therapy in platinum-sensitive relapsed ovarian cancer. *N Engl J Med* 2012;366:1382–92.
- Ahmed AA, Etemadmoghadam D, Temple J, Lynch AG, Riad M, Sharma R, et al. Driver mutations in TP53 are ubiquitous in high grade serous carcinoma of the ovary. *J Pathol* 2010;221:49–56.
- Cancer Genome Atlas Research Network. Integrated genomic analyses of ovarian carcinoma. *Nature* 2011;474:609–15.
- Patch AM, Christie EL, Etemadmoghadam D, Garsed DW, George J, Fereday S, et al. Whole-genome characterization of chemoresistant ovarian cancer. *Nature* 2015;521:489–94.
- Scott CL, Swisher EM, Kaufmann SH. Poly (ADP-ribose) polymerase inhibitors: recent advances and future development. *J Clin Oncol* 2015;33:1397–406.
- Etemadmoghadam D, deFazio A, Beroukhim R, Mermel C, George J, Getz G, et al. Integrated genome-wide DNA copy number and expression analysis identifies distinct mechanisms of primary chemoresistance in ovarian carcinomas. *Clin Cancer Res* 2009;15:1417–27.
- Nakayama N, Nakayama K, Shamima Y, Ishikawa M, Katagiri A, Iida K, et al. Gene amplification CCNE1 is related to poor survival and potential therapeutic target in ovarian cancer. *Cancer* 2010;116:2621–34.
- Etemadmoghadam D, Weir BA, Au-Yeung G, Alsop K, Mitchell G, George J, et al. Synthetic lethality between CCNE1 amplification and loss of BRCA1. *Proc Natl Acad Sci U S A* 2013;110:19489–94.
- Etemadmoghadam D, Au-Yeung G, Wall M, Mitchell C, Kansara M, Loehrer E, et al. Resistance to CDK2 inhibitors is associated with selection of polyploid cells in CCNE1-amplified ovarian cancer. *Clin Cancer Res* 2013;19:5960–71.
- Ellis LM, Hicklin DJ. Resistance to targeted therapies: refining anticancer therapy in the era of molecular oncology. *Clin Cancer Res* 2009;15:7471–8.
- Yap TA, Omlin A, de Bono JS. Development of therapeutic combinations targeting major cancer signaling pathways. *J Clin Oncol* 2013;31:1592–605.
- Fitzgerald JB, Schoeberl B, Nielsen UB, Sorger PK. Systems biology and combination therapy in the quest for clinical efficacy. *Nat Chem Biol* 2006;2:458–66.
- Parry D, Guzi T, Shanahan F, Davis N, Prabhavalkar D, Wiswell D, et al. Dinaciclib (SCH 727965), a novel and potent cyclin-dependent kinase inhibitor. *Mol Cancer Ther* 2010;9:2344–53.
- Fellmann C, Hoffmann T, Sridhar V, Hopfgartner B, Muhar M, Roth M, et al. An optimized microRNA backbone for effective single-copy RNAi. *Cell Rep* 2013;5:1704–13.
- Karst AM, Jones PM, Vena N, Ligon AH, Liu JF, Hirsch MS, et al. Cyclin E1 deregulation occurs early in secretory cell transformation to promote formation of fallopian tube-derived high-grade serous ovarian cancers. *Cancer Res* 2014;74:1141–52.
- Astle MV, Hannan KM, Ng PY, Lee RS, George AJ, Hsu AK, et al. AKT induces senescence in human cells via mTORC1 and p53 in the absence of DNA damage: implications for targeting mTOR during malignancy. *Oncogene* 2012;31:1949–62.
- Lackovic K, Lessene G, Falk H, Leuchowius KJ, Baell J, Street I. A perspective on 10-years HTS experience at the walter and eliza hall institute of medical research - eighteen million assays and counting. *Comb Chem High Throughput Screen* 2014;17:241–52.
- Cerami E, Gao J, Dogrusoz U, Gross BE, Sumer SO, Aksoy BA, et al. The cBio cancer genomics portal: an open platform for exploring multidimensional cancer genomics data. *Cancer Discov* 2012;2:401–4.
- Gao J, Aksoy BA, Dogrusoz U, Dresdner G, Gross B, Sumer SO, et al. Integrative analysis of complex cancer genomics and clinical profiles using the cBioPortal. *Sci Signal* 2013;6:p11.
- Cowley GS, Weir BA, Vazquez F, Tamayo P, Scott JA, Rusin S, et al. Parallel genome-scale loss of function screens in 216 cancer cell lines for the identification of context-specific genetic dependencies. *Sci Data* 2014;1:140035.
- Barretina J, Caponigro G, Stransky N, Venkatesan K, Margolin AA, Kim S, et al. The cancer cell line encyclopedia enables predictive modelling of anticancer drug sensitivity. *Nature* 2012;483:603–7.
- Domcke S, Sinha R, Levine DA, Sander C, Schultz N. Evaluating cell lines as tumour models by comparison of genomic profiles. *Nat Commun* 2013;4:2126.
- Shapiro G. Beyond CDK4/6: Targeting additional cell cycle and transcriptional CDKs in breast cancer [abstract]. In: Proceedings of the Thirty-Eighth Annual CTCR-AACR San Antonio Breast Cancer Symposium; 2015 Dec 8–12; San Antonio, TX. Philadelphia (PA): AACR. Abstract nr MS1–1.
- Chou TC. Drug combination studies and their synergy quantification using the Chou-Talalay method. *Cancer Res* 2010;70:440–6.
- Gojo I, Zhang B, Fenton RG. The cyclin-dependent kinase inhibitor flavopiridol induces apoptosis in multiple myeloma cells through transcriptional repression and down-regulation of Mcl-1. *Clin Cancer Res* 2002;8:3527–38.
- Geng Y, Lee YM, Welcker M, Swanger J, Zagodzdon A, Winer JD, et al. Kinase-independent function of cyclin E. *Mol Cell* 2007;25:127–39.
- Horiuchi D, Huskey NE, Kusdra L, Wohlbold L, Merrick KA, Zhang C, et al. Chemical-genetic analysis of cyclin dependent kinase 2 function reveals an important role in cellular transformation by multiple oncogenic pathways. *Proc Natl Acad Sci U S A* 2012;109:E1019–27.
- Echalier A, Cot E, Camasses A, Hodimont E, Hoh F, Jay P, et al. An integrated chemical biology approach provides insight into Cdk2 functional redundancy and inhibitor sensitivity. *Chem Biol* 2012;19:1028–40.
- Asghar U, Witkiewicz AK, Turner NC, Knudsen ES. The history and future of targeting cyclin-dependent kinases in cancer therapy. *Nat Rev Drug Discov* 2015;14:130–46.
- Anglesio MS, Wiegand KC, Melnyk N, Chow C, Salamanca C, Prentice LM, et al. Type-specific cell line models for type-specific ovarian cancer research. *PLoS ONE* 2013;8:e72162.
- Beaufort CM, HelmiJR JC, Piskorz AM, Hoogstraat M, Ruigrok-Ritsier K, Besselink N, et al. Ovarian cancer cell line panel (OCCP): clinical importance of *invitro* morphological subtypes. *PLoS ONE* 2014;9:e103988.
- Elias KM, Emori MM, Papp E, MacDuffie E, Konecny GE, Velculescu VE, et al. Beyond genomics: critical evaluation of cell line utility for ovarian cancer research. *Gynecol Oncol* 2015;139:97–103.
- Hu C, Dadon T, Chenna V, Yabuuchi S, Bannerji R, Booher R, et al. Combined inhibition of cyclin-dependent kinases (Dinaciclib) and AKT (MK-2206) blocks pancreatic tumor growth and metastases in patient-derived xenograft models. *Mol Cancer Ther* 2015;14:1532–9.